

# Piezoelectric Hydrogels: Hybrid Material Design, Properties, and Biomedical Applications

Chi Zhang, Sun Hwa Kwon, and Lin Dong\*

**Hydrogels show great potential in biomedical applications due to their inherent biocompatibility, high water content, and resemblance to the extracellular matrix. However, they lack self-powering capabilities and often necessitate external stimulation to initiate cell regenerative processes. In contrast, piezoelectric materials offer self-powering potential but tend to compromise flexibility. To address this, creating a novel hybrid biomaterial of piezoelectric hydrogels (PHs), which combines the advantageous properties of both materials, offers a systematic solution to the challenges faced by these materials when employed separately. Such innovative material system is expected to broaden the horizons of biomedical applications, such as piezocatalytic medicinal and health monitoring applications, showcasing its adaptability by endowing hydrogels with piezoelectric properties. Unique functionalities, like enabling self-powered capabilities and inducing electrical stimulation that mimics endogenous bioelectricity, can be achieved while retaining hydrogel matrix advantages. Given the limited reported literature on PHs, here recent strategies concerning material design and fabrication, essential properties, and distinctive applications are systematically discussed. The review is concluded by providing perspectives on the remaining challenges and the future outlook for PHs in the biomedical field. As PHs emerge as a rising star, a comprehensive exploration of their potential offers insights into the new hybrid biomaterials.**

properties. These materials aim to facilitate the fabrication process and enhance applicability in the biomedical field.<sup>[10–13]</sup> Commonly used materials exhibit some but not all the properties, and as such, the resulting biomedically engineered device can consist of various functional components to establish multifunctionality, which can result in making the device bulky, rigid, and not conformable to the human body. To address such challenges, a novel material system termed as the piezoelectric hydrogel (PH) has been developed to integrate various desirable properties for use in biomedical applications. This hybrid biomaterial has significant advantages that demonstrate multiple functions, which expand the range of applications to include cell regenerative techniques and health monitoring processes. Additionally, the PH-based device safely delivers robust cellular structural support and long-term solutions by exhibiting flexibility, biocompatibility, and even biodegradability while also enabling self-induced electrical stimulation that mimics endogenous bioelectricity, henceforth systematically presented in this review.<sup>[14,15]</sup>

For biomedical applications, hydrogels are commonly employed biomaterials that

are soft, flexible, and biocompatible, and they can also maintain high water contents, which allow them to achieve a strong similarity to the extracellular matrix (ECM).<sup>[16–20]</sup> Additional advantageous properties, such as tunable biodegradability and bioadhesion, make them excellent cell carriers/matrices and delivery vehicles for biomolecules and drugs as well, with the ability to retain drugs for an extended period of time before delivering them to the target location within the body.<sup>[16,21–23]</sup> Furthermore, through nanomaterial functionalization, hydrogels can achieve responsiveness to various stimuli such as pH, temperature, magnetic fields, and chemical stimuli.<sup>[16–23]</sup> However, despite having such responsiveness, traditional and pristine hydrogels are incapable of providing stimuli on their own without an additional functional component and are unable to solely initiate regenerative processes like cell regeneration, which requires endogenous bioelectric stimulation.<sup>[24–27]</sup> Additionally, most biomedical devices that use pristine hydrogels as their functional material require a separate power source for operation, consequently making the overall device rigid and bulky. In contrast, piezoelectric materials are another class of materials that can be utilized in a

## 1. Introduction

Over the past several decades, biomaterials have been revolutionizing the discipline of biomedical engineering by instigating the restoration and recovery of the biological function of a patient's damaged tissues or organs for use in crucial applications such as tissue engineering.<sup>[1–9]</sup> In recent years, the trajectory for human discovery and development has shifted towards a rapid progress towards technological advancement. This has led to a pressing need for biomaterials with structures resembling biological tissues, capable of exhibiting novel and multifunctional

---

C. Zhang, S. H. Kwon, L. Dong  
Department of Mechanical and Industrial Engineering  
New Jersey Institute of Technology  
Newark, NJ 07114, USA  
E-mail: [lin.dong@njit.edu](mailto:lin.dong@njit.edu)

 The ORCID identification number(s) for the author(s) of this article can be found under <https://doi.org/10.1002/smll.202310110>

DOI: 10.1002/smll.202310110

variety of engineering disciplines, including the biomedical engineering field, due to their unique ability to convert mechanical stress into electricity.<sup>[28–30]</sup> Piezoelectric materials are mainly categorized into ceramics, single crystals, and polymers, with each category having its own advantages and disadvantages. Piezoelectric ceramics such as barium titanate (BTO) demonstrate excellent piezoelectric and dielectric properties; however, these ceramics are very rigid, brittle, and are not completely biosafe.<sup>[31–33]</sup> For piezoelectric single crystals, their crystallographic axes govern the material quality and initial material purity, but single crystals display a wide range of piezoelectricity, with quartz displaying weaker piezoelectric properties when compared to piezoelectric ceramics whereas lead magnesium niobate-lead titanate displays much higher piezoelectricity.<sup>[28,34]</sup> As for piezoelectric polymers such as poly(vinylidene fluoride) (PVDF), they are flexible, lightweight, and biocompatible, which are all desirable properties in the biomedical field.<sup>[35–38]</sup> When compared to their ceramic counterparts, however, they display weaker piezoelectric properties. Overall, piezoelectric materials are generally more rigid and not as flexible when compared to hydrogels that are more commonly employed in biomedical applications, and not all piezoelectric materials are biocompatible, making it particularly difficult for pristine piezoelectric materials to be utilized in biomedical applications. Hence, they commonly require further design strategies or integration with other materials to take full advantage of their piezoelectric properties in the field.<sup>[39–43]</sup>

In light of this, the development of a novel hybrid material system by combining both hydrogels and piezoelectricity is of great interest to the field as an emerging new material due to the integration of the advantageous properties of both classes of materials. The highly tunable performance of PHs can realize specific functions, such as self-inducing electrical stimulation that mimics endogenous bioelectricity at localized areas to initiate cell regenerative processes and self-powering the overall device. They also simultaneously retain the properties of the overall hydrogel matrix, like inherent biocompatibility, tunable biodegradability, and excellent flexibility. Furthermore, PHs contribute to a broader range of applicability to include piezocatalytic medicine alongside tissue engineering and health monitoring applications. This new application within the biomedical field relies on the ability of hybridized piezoelectric materials to release free electrons under a strain state to generate reactive oxygen species (ROS) for cancer or antibacterial therapeutic purposes while piezoelectric materials alone have difficulty acting as the sole medicinal carriers.<sup>[44–48]</sup> As such, PHs have demonstrated immense potential and capability in the biomedical field by integrating two separate material classes of pristine hydrogels and pristine piezoelectric materials by endowing hydrogels with piezoelectric properties. Despite showing such promise within this field, it is not yet widely studied and many challenges exist, such as complex pre-processing techniques and insufficient bioelectrical stimulation. Moreover, the overall flexibility of PHs is determined by the flexibility of the hydrogel matrix whereas the piezoelectricity of PHs is contingent on the quantity of integrated piezoelectric materials. Thus, it is crucial to strike a good balance to effectively harness the advantageous properties of both materials. Therefore, a deeper understanding of this hybrid class of materials is imperative to advance and promote the utilization of PHs in biomedical applications. To the best of the authors' knowl-

edge, the topic of this emerging new biomaterial is lacking comprehensive understanding.

In this review, we highlight recent advances in PHs, herein categorized into natural biopolymer hydrogels and synthetic polymer hydrogels, and their applications in the biomedical engineering field, which is consequently summarized in **Figure 1**. We begin by discussing the recent strategies for material design and fabrication of PHs, either based on natural biopolymer hydrogels or synthetic polymer hydrogels. Then, the properties of PHs that are crucial to the biomedical engineering field are explored, such as the piezoelectricity, flexibility, biocompatibility, and biodegradability. Next, specific applications utilizing PHs within the field are reviewed in great detail, in which the use of PHs is categorized into wound healing and tissue regeneration, piezocatalytic medicine, and health and motion monitoring. Lastly, we conclude by providing a summary of perspectives regarding PH composites that are used in the biomedical engineering field. Beyond these discussions, this review emphasizes the advantages of employing this innovative material system over each individual class of materials separately. The scope of this review emphasizes the potentiality of PHs, which can facilitate new discussions and research to further progress the use of this novel hybrid material system.

## 2. Design Strategies and Fabrication Methods of Piezoelectric Hydrogels

The realization of PHs relies on the rational design of introducing piezoelectric materials into a hydrogel matrix. In most circumstances, piezoelectric components are not directly involved in the crosslinking of hydrogels. Therefore, achieving successful interactions between piezoelectric components and hydrogel polymer chains are of great importance to integrate them into 3D-interconnected networks. Through the combination of different piezoelectric materials and hydrogel systems, a variety of PHs can be developed with desired formats and structures. Here, we classify the design of PHs into two categories based on the utilized hydrogel matrix: natural biopolymer hydrogels and synthetic polymer hydrogels.

### 2.1. Utilizing Natural Biopolymer Hydrogels

Natural biopolymer hydrogels have attracted great interest in biomedical applications such as tissue regeneration, drug delivery, and medical implants due to their inherent biocompatibility and close resemblance to the ECM.<sup>[49–55]</sup> In addition, because of the intrinsic asymmetry in crystal structures that give rise to the piezoelectric effect, the majority of natural biopolymers exhibit significant potential for PH fabrication. For example, one of the most common natural biopolymers favorable for PH fabrication is silk fibroin (SF), which can be easily derived from silkworm, spiders, or other sources in nature. Owing to its naturally superior biocompatibility and biodegradability, SF has been widely studied as an environmentally friendly “green” biopolymer.<sup>[56–59]</sup> Although the composition of SF obtained from different species differs, the different types of SFs share similar structures, i.e., long amino acid chains consisting

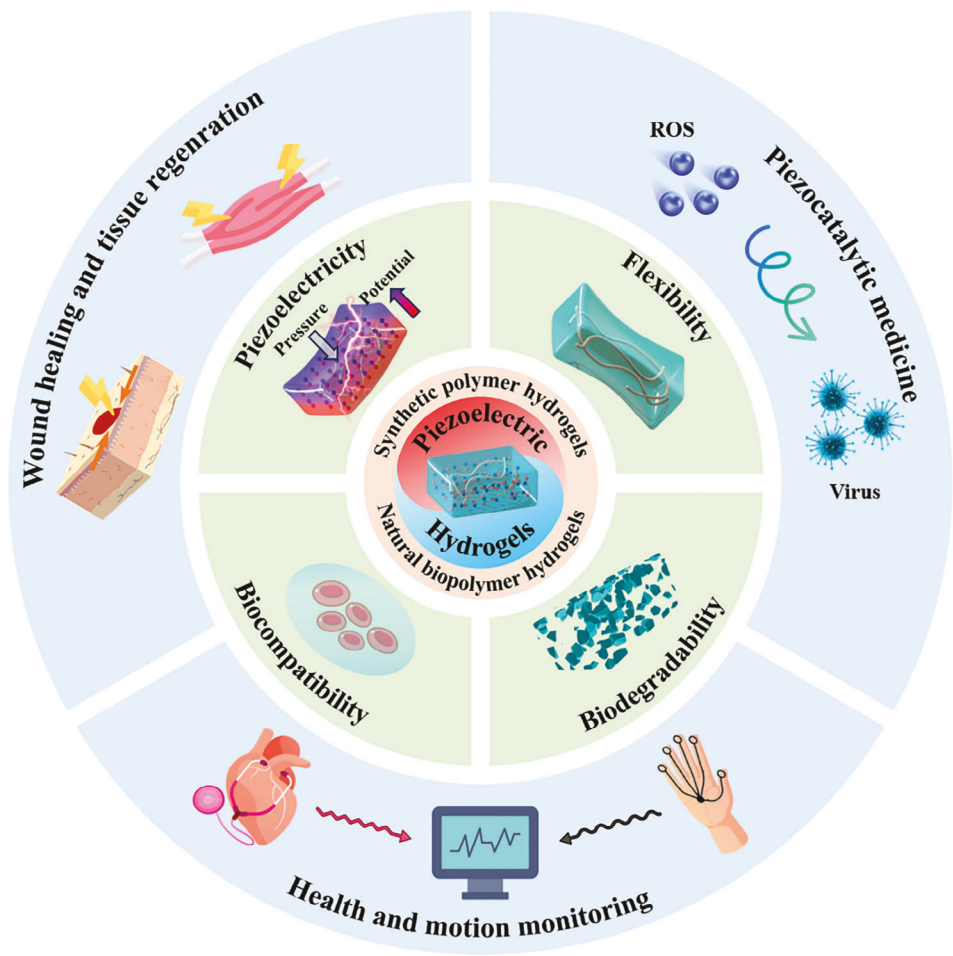


**Figure 1.** A schematic overview of the PH material system regarding the design strategies, key properties, and its utilization in the field of biomedical applications.

of repetitive crystalline hydrophobic domains and noncrystalline hydrophilic domains, which form secondary structures including  $\alpha$ -helices,  $\beta$ -sheets, and random coils.<sup>[60]</sup> Among those secondary structures, the highly crystalline  $\beta$ -sheets are formed between hydrophobic domains through multiple interactions such as hydrogen bonds, van der Waals forces, and hydrophobic interactions, contributing to remarkable mechanical robustness of SF.<sup>[61]</sup> Moreover, the  $\beta$ -sheet structure endows SF with intrinsic piezoelectricity ( $d_{14} \approx -1.5 \text{ pC N}^{-1}$ ) depending on its  $\beta$ -sheet crystallinity and crystalline orientation,<sup>[62]</sup> making it a promising candidate for developing biopolymer-based PHs. The gelation of SF is generally through inter- or intra-molecular interactions of the long SF molecular chains, including hydrophobic interactions and hydrogen bonding, which crosslink those molecular chains. When external factors, such as electric fields,<sup>[63]</sup> UV irradiation,<sup>[64]</sup> and ultrasonic treatment,<sup>[65]</sup> are applied, they facilitate the interactions between the SF molecular chains, thus leading to a rapid crosslinking of these chains, through which SF hydrogels are obtained. Additionally, those external factors have been proven to promote the structure transition from random coils to  $\beta$ -sheets, resulting in excellent mechanical stability as well as effective piezoelectric response of SF hydrogels.<sup>[56,60]</sup>

Different fabrication methods have been reported to develop natural biopolymer hydrogels, such as SF hydrogels. For example, Chouhan et al. developed SF hydrogel formulation by incubating a blend solution of two different SF proteins at 37 °C.<sup>[66]</sup> In this approach, *Bombyx mori* SF (BmSF) and *Antheraea assama* SF (AaSF), isolated from two sources, were mixed together to trigger the self-assembly of SF molecular chains to produce a highly crosslinked SF hydrogel with the formation of  $\beta$ -sheet structures, as shown in Figure 2a. The mechanism of the self-assembly between two SF molecular chains was investigated. Briefly, BmSF and AaSF had variations in hydrophobicity and hydrophilicity due to their different amino acid sequences, which attributed to the inherent self-assembly between them. With the synergistic effect of hydrophobic interaction and hydrogen bonding, the transparent blend solution eventually transformed into an opaque hydrogel. In another research, a binary-solvent-induced conformation transition (BSICT) method for preparing SF hydrogels was reported.<sup>[67]</sup> The formation of SF hydrogel was induced by sequentially adding two different solvents to pristine SF. Such BSICT-SF hydrogels were prepared into versatile 3D shapes with different material formats, which was colored through blending with different inorganic and organic dyes. Moreover,

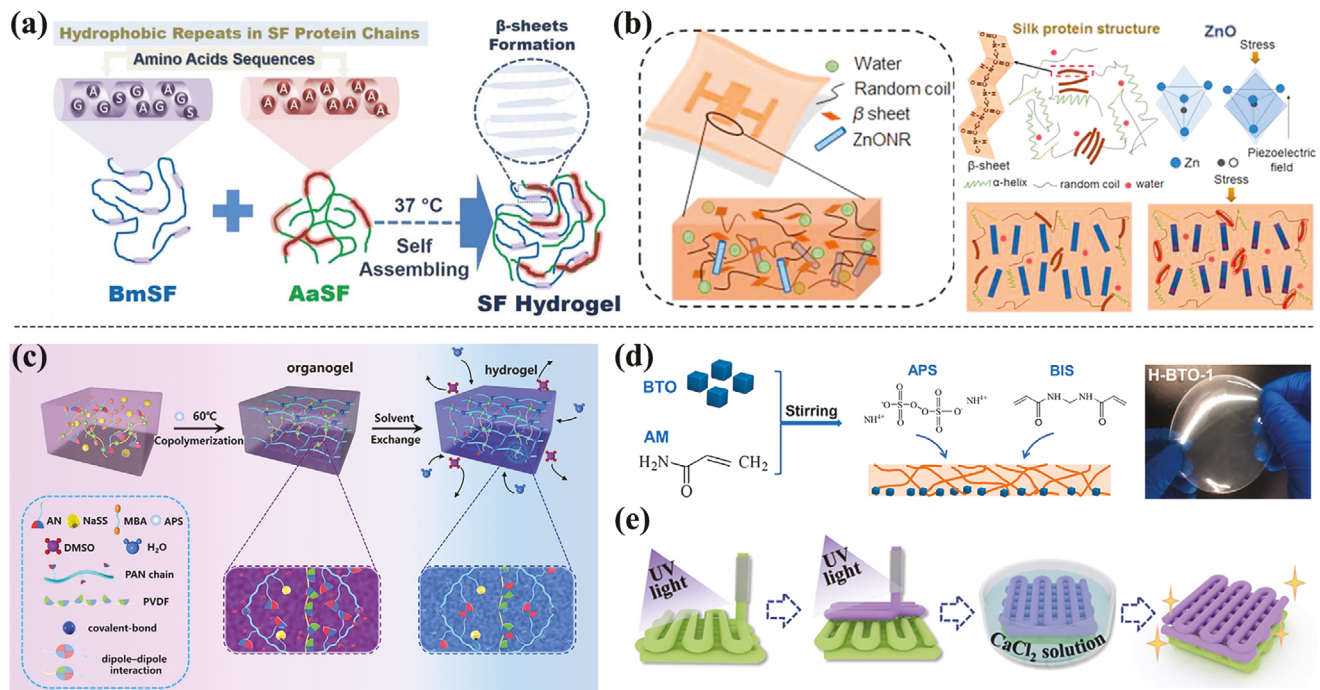


**Figure 2.** Material design strategies for PHs by utilizing a,b) natural biopolymer hydrogels and c–e) synthetic polymer hydrogels. a) Schematic formulation of the SF hydrogel through a self-assembly approach. Reproduced with permission.<sup>[66]</sup> Copyright 2018, Wiley. b) Illustration of the design of SF/ZnONRs hydrogel and its piezoelectric mechanism. Reproduced with permission.<sup>[68]</sup> Copyright 2020, Elsevier. c) Formulation process of the PAN-PVDF hydrogel. Reproduced with permission.<sup>[75]</sup> Copyright 2019, American Chemical Society. d) The fabrication process of the BTO composite hydrogel film. Reproduced with permission.<sup>[76]</sup> Copyright 2022, American Chemical Society. e) Development of a Janus PH patch by 3D printing method. Reproduced with permission.<sup>[77]</sup> Copyright 2023, AAAS.

SF-based composite hydrogels can be developed by introducing inorganic piezoelectric materials into the SF solution. For example, Gogurla et al. reported a nanocomposite PH comprised of SF and zinc oxide nanorods (ZnONRs).<sup>[68]</sup> The SF/ZnONRs hydrogel was formed via a simple solution casting process, during which SF molecular chains and ZnONRs were interconnected (Figure 2b). SF  $\beta$ -sheets and ZnONRs were able to generate piezoelectric potential resulting from individual dipole movements under mechanical stress. For the composite hydrogel system, coupled dipole movements occurred due to the piezoelectric coupling effect and ultimately contributed to an increased piezoelectric field.

In addition to SF, other natural biopolymers, such as chitin,<sup>[69]</sup> chitosan,<sup>[70]</sup> collagen,<sup>[71]</sup> and bacterial cellulose,<sup>[72]</sup> have also been reported for PH development. Due to their intrinsic piezoelectricity, PHs can be obtained from those biopolymers simply through self-assembly or sol-gel process without using other piezoelectric materials. Natural biopolymer-based PHs are favorable for biomedical engineering applications, since they are directly derived from living organisms and can be naturally compatible with biological tissues without causing immune rejection.<sup>[73]</sup> Another significant advantage of using natural biopolymers for PH fabrication is to utilize their biodegradability. For example, the biodegradation rate of SF can be programmed to be controlled from hours to years by changing the external factors to adjust its  $\beta$ -sheet content and the organization degree of amorphous domains.<sup>[74]</sup> Moreover, the gelation of these biopolymers usually relies on inter- or intra-molecular interactions to form

physical crosslinks and no additional crosslinking agents are required in this process, thus effectively avoiding the introduction of toxic or difficult-to-degrade chemical components. However, despite such advantages, the development of natural biopolymer-based PHs is still hindered by their relatively low piezoelectricity, random piezoelectric phase orientation, and complex pre-processing. While the introduction of other piezoelectric materials provides a feasible option, achieving effective interactions between those materials and biopolymers, which are essential for a composite hydrogel system, proves to be challenging. Therefore, future efforts will be directed toward emphasizing these aspects for the development of composite hydrogel systems.

## 2.2. Utilizing Synthetic Polymer Hydrogels

In addition to natural polymer hydrogels, synthetic polymer hydrogels have been extensively studied due to their high gelation strength, long lifespan, ease of processing, and good adaptability.<sup>[78,79]</sup> In order to cater to specific requirements for various applications, significant efforts have been made in the development of functionalized hydrogels based on synthetic polymers such as polyacrylamide (PAM), polyacrylonitrile (PAN), and polyvinyl alcohol (PVA).<sup>[80–84]</sup> By combining piezoelectric materials with those polymers in a hydrogel matrix, PHs can be easily fabricated with designed compositions and structures. Unlike physically crosslinked biopolymer-based PHs, those developed from synthetic polymers typically employ chemical crosslinking

methods that hinge on the bonding between hydrogel polymer chains. To create such chemical crosslinking, crosslinking agents carrying functional groups are introduced to react with certain functional groups on the polymer chains, thus serving as bridges to connect those polymer chains. Furthermore, it is possible to introduce specific interactions between hydrogel polymer chains and piezoelectric components to achieve a homogeneous composite system.

So far, both organic and inorganic piezoelectric materials have been incorporated as the piezoelectric functional components of synthetic polymer-based PHs. PVDF is the most widely used piezoelectric polymer because of its relatively high piezoelectric response ( $d_{33} = -33 \text{ pC N}^{-1}$ ), good flexibility, and easy processing.<sup>[85,86]</sup> The challenge of introducing PVDF into a hydrogel comes from its natural hydrophobic nature, which makes it hard to be stabilized in a hydrophilic hydrogel matrix. To overcome such a challenge, polar organic solvents such as dimethyl sulfoxide (DMSO) can be utilized to provide a homogeneous organogel matrix, where the crosslinking of PVDF and organogel polymer chains occurs, and hydrogels can be subsequently obtained through the solvent exchange. For example, Fu et al. reported the fabrication of a PAN-PVDF hydrogel based on the DMSO matrix.<sup>[75]</sup> As shown in Figure 2c, the PAN-PVDF organogel was first formed in a mixed DMSO solution, where polymerized PAN was crosslinked by methylenebisacrylamide (MBA) while PVDF and PAN were combined by dipole–dipole interaction, and then the PAN-PVDF hydrogel was obtained through a solvent exchange process. The introduced dipole–dipole interaction not only helped to stabilize PVDF in the hydrogel matrix, but also contributed to a significant increase of its piezoelectric  $\beta$ -phase content. In addition, a PVA/PVDF hydrogel was developed using similar method, in which PVA and PVDF were crosslinked in DMSO matrix via strong hydrogen bonding.<sup>[87]</sup> After solvent exchange, the hydrogel was further treated through an annealing-swelling process to promote the transition of the  $\alpha$ -phase of PVDF to the  $\beta$ -phase. For inorganic piezoelectric materials, a promising candidate for synthetic PH fabrication is BTO, a well-known piezoelectric ceramic with high piezoelectricity ( $d_{33} = 190 \text{ pC N}^{-1}$ ), good biocompatibility, and ease of synthesis.<sup>[88,89]</sup> Currently, remarkable progress has been achieved in developing synthetic PHs loaded with BTO. For example, Wang et al. developed a BTO composite hydrogel film by introducing BTO nanocubes into a PAM hydrogel.<sup>[76]</sup> The PAM chains were chemically crosslinked while no interactions formed between BTO and PAM, resulting in an asymmetric distribution of BTO nanocubes on one side of the hydrogel film (Figure 2d). Similar results were reported in another composite PH comprised of poly(vinyl pyrrolidone), poly(ethylene glycol), and BTO nanoparticles, where the agglomeration of BTO nanoparticles occurred as the water content of the hydrogel increased.<sup>[90]</sup> Typically, BTO nanoparticles are difficult to be uniformly dispersed in hydrogel matrix due to their high weight and lack of interactions with polymer chains. To address this issue, specific interactions between BTO nanoparticles and polymer chains are required. Recently, a multicrosslinked PH composite based on surface-aminated BTO (ABTO) nanoparticles, oxidized chondroitin sulfate (OCS), gelatin (Gel), and boric acid was reported.<sup>[91]</sup> The surface amino functionalization of BTO improved its dispersibility and meanwhile enabled chemical bond-

ing with OCS chains. Besides the crosslinking formed between polymer chains, ABTO nanoparticles also acted as crosslinking sites during hydrogel formation. Such interactions contributed to a uniform distribution of ABTO nanoparticles in the hydrogel matrix. While the aforementioned strategies for developing PHs are based on conventional hydrogel formats, i.e., bulks or films, PHs can also be fabricated into customized 3D structures by the 3D printing method using synthetic polymers. For example, Huang et al. used 3D printing to fabricate a Janus PH patch with two-layer hydrogel meshes.<sup>[77]</sup> As shown in Figure 2e, two photo-crosslinkable layers of methacrylate gelatin (GelMA) hydrogels and poly(ethylene glycol) diacrylate (PEGDA) hydrogels loaded with BTO particles were printed under ultraviolet light (UV) exposure to form a UV-crosslinked hydrogel patch, which was subsequently immersed in  $\text{CaCl}_2$  solution to initiate ionic crosslinking. By combining two types of crosslinking, a Janus PH patch with excellent mechanical integrity as well as a stable mesh structure was obtained. In another case, ZnO nanoparticles modified PVDF/sodium alginate (SA) PH scaffold was developed by utilizing bioink 3D printing.<sup>[25]</sup> The bioink, prepared through dissolving ZnO modified PVDF and SA in water/dimethylformamide (DMF) co-solvent, was printed into a hydrogel precursor and subsequently crosslinked by  $\text{Ca}^{2+}$  to form the PH scaffold.

Overall, the development of PHs can be achieved through the incorporation of either organic or inorganic piezoelectric materials into synthetic polymer hydrogels. Different strategies can be adopted to obtain interactions between those piezoelectric components and polymer chains within the hydrogel. On one hand, surface modification techniques can be employed to decorate piezoelectric particles with a variety of functional groups that have the ability to form chemical bonding with polymer chains of the hydrogel. On the other hand, physical interactions such as hydrogen bonding and dipole–dipole interaction provide additional options for designing the polymer chains within the hydrogel. Furthermore, it is worth noting that 3D printing offers a convenient method to create PHs with tailored 3D structures. This capability proves challenging to achieve when dealing with hydrogels based on natural biopolymers. Hence, the utilization of synthetic polymers opens up multiple avenues for developing PHs with diverse compositions and structures. Nevertheless, these fabricated PHs from synthetic polymers are non-biodegradable, potentially raising concerns about recycling.

In this section, we overview recent development of PHs regarding their material designs and fabrication methods and also highlight their advantages and disadvantages, as summarized in Table 1. The designs of PHs are classified into two categories based on the types of hydrogel matrix: natural biopolymers and synthetic polymers. For natural biopolymer-based PHs, those polymers not only contribute to the hydrogel networks, but also serve as piezoelectric functional components due to their inherent piezoelectricity. However, due to the low levels of the inherent piezoelectricity, additional piezoelectric components are often introduced to improve the piezoelectric response, which might affect the gelation strength of the hydrogel matrix. Such PHs can be obtained by physical crosslinking through different and sometimes complex solution processing methods with little or no extra chemical usage, thus providing a biological environment with excellent biocompatibility and high similarity to the ECM. As for PHs based on synthetic polymers, various

**Table 1.** A summary of the material designs and fabrication methods of representative PHs.

| Hydrogel matrix     | Advantages and disadvantages  | Hydrogel networks   | Piezoelectric components | Fabrication methods                   | Crosslinking methods  | Refs. |
|---------------------|---|---------------------|--------------------------|---------------------------------------|-----------------------|-------|
| Natural biopolymers | <ul style="list-style-type: none"> <li>• Similarity to ECM</li> <li>• Little or no toxicity</li> <li>• Biodegradability</li> <li>• Low gelation strength</li> <li>• Low piezoelectricity</li> <li>• Complex processing</li> </ul> | SF                  | SF                       | Sol-gel                               | Physical              | [66]  |
|                     |   | SF                  | SF, ZnONRs               | Solution casting                      | Physical              | [68]  |
|                     |   | SF                  | SF, BTO                  | Sol-gel                               | Chemical              | [92]  |
|                     |   | Chitosan            | Chitosan                 | Solution casting                      | Physical and chemical | [70]  |
|                     |   | Bacterial cellulose | Imidazolium perchlorate  | Incubation and infiltration           | Physical              | [72]  |
|                     |   | PAN                 | PVDF                     | Sol-gel and solvent exchange          | Physical and chemical | [75]  |
| Synthetic polymers  | <ul style="list-style-type: none"> <li>• High gelation strength</li> <li>• High piezoelectricity</li> <li>• Easy processing</li> <li>• Nonbiodegradability</li> </ul>   | PAM                 | BTO                      | Sol-gel                               | Chemical              | [76]  |
|                     |   | PAN/ PAM            | PVDF                     | Sol-gel and solvent exchange          | Physical and chemical | [93]  |
|                     |   | PVA                 | PVDF                     | Freezing/thawing and solvent exchange | Physical              | [87]  |
|                     |   | GelMA/ PEGDA        | BTO                      | 3D printing                           | Chemical              | [77]  |
|                     |   | SA                  | PVDF                     | 3D printing                           | Chemical              | [25]  |

combinations of the hydrogel matrix and piezoelectric components can be developed via a simple sol-gel process or even 3D printing methods, enabling controllable and scalable fabrication of PHs. Due to the existence of more crosslinking sites with the introduced piezoelectric materials, PHs utilizing synthetic polymers are usually obtained with higher gelation strength and piezoelectricity. However, those PHs would not be considered fully biocompatible or biodegradable, which may hinder their applicability in the biomedical field. Ultimately, through rational design strategies and fabrication methods, the integration of hydrogels and piezoelectric materials has been realized in a novel material system, namely the PHs. It is expected that the PHs will exhibit multiple combination properties desirable for biomedical applications.

### 3. Key Properties of Piezoelectric Hydrogels in Biomedical Applications

PHs are favorable in the field of biomedical applications owing to their integrated properties from both hydrogels and piezoelectric materials (Figure 3). On one hand, hydrogels are flexible and able to generate reversible deformation under external pressures while exhibiting excellent biocompatibility and tunable biodegradability, which make them ideal for wearing or implanting in the body. However, pristine hydrogels are unable to initiate cell regeneration, a critical aspect for wound healing and tissue engineering applications, without external stimulation. On the other hand, piezoelectric materials can generate electrical potentials due to the piezoelectric effect; however, most of these materials are rigid and have poor deformability, making it challenging for *in vivo* applications. Therefore, through integrating hydrogels

and piezoelectric materials in one material system as PHs, the advantageous properties of each can be combined and utilized in biomedical applications. First of all, PHs inherit flexibility from hydrogels and piezoelectricity from piezoelectric materials. The mechanical-electrical response of PHs is illustrated in Figure 3. Without stress, the dipoles inside the PH are randomly oriented and the net dipole moment is zero, thus no potential is generated. When an external pressure is applied on the PH, those dipoles will be aligned along with the deformation of the PH, resulting in a net dipole moment change and the generation of a piezoelectric potential. Once the external pressure is released, the PH recovers to its original state and those dipoles become randomly oriented again with the potential difference back to zero. Furthermore, PHs also exhibit excellent biocompatibility owing to the biocompatible nature of hydrogels, ensuring their safe and direct contact with the human skin or biological tissues. In addition, certain PHs that utilize natural biopolymers are capable of biodegradation and show promise for recycling. In this section, we provide a comprehensive overview and summary of key properties such as piezoelectricity, flexibility, biocompatibility, and biodegradability, which are associated with PHs in biomedical applications.

#### 3.1. Piezoelectric Performance of PHs

The intricate nature and diversity of living organisms impose precise criteria on the piezoelectric performance of PHs in the context of their applications in biomedical engineering. For example, in wound healing applications, the electrical output of PHs is required to be enough to match the wound's endogenous electric field.<sup>[94]</sup> For motion and health monitoring, PHs work as

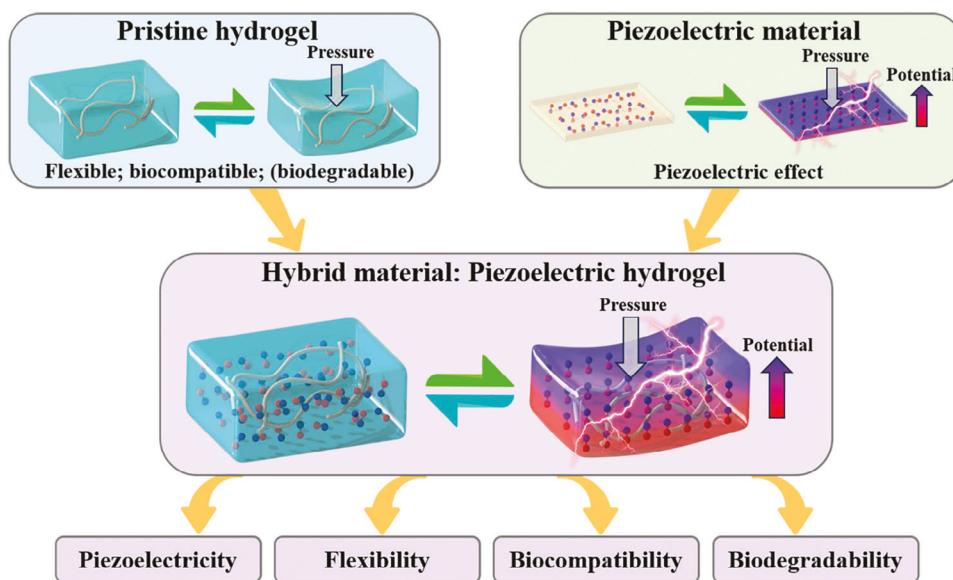


**Figure 3.** Schematic illustration of the key properties of pristine hydrogel, the piezoelectric material, and the hybrid material (PH) in biomedical applications. Insets are the schematic illustration of their mechanical-electrical response when subject to external pressure.

sensors to respond to various stimuli such as pressure, pulse, vocal cord vibration, and more, thus converting biological signals into electrical signals.<sup>[30]</sup> The majority of stimuli encountered in daily life exhibit low intensity, leading to minimal mechanical input of PHs. Therefore, the sensitivity of PHs is crucial, necessitating their capability to detect subtle stimuli and generate piezoelectricity to ensure precise monitoring. Furthermore, the piezoelectric durability of PHs is also of significant importance. Given that both biomedical monitoring and treatment are extended processes, it is essential for PHs to maintain a consistent and stable piezoelectric performance over an extended period of time.

Comprehensive studies have been conducted in evaluating the piezoelectric performance of PHs. For example, Gogurla et al. assembled the SF/ZnONRs hydrogel with two silver nanowire electrodes into a PH device (Figure 4a) and investigated its piezoelectric response.<sup>[68]</sup> The electrical output of the PH device increased significantly after introducing ZnONRs into the SF hydrogel due to the piezoelectric coupling effect between ZnONRs and SF  $\beta$ -sheets. By attaching the PH device on a finger, it was able to generate piezoelectric responses to slight stress changes during finger bending and relaxing (Figure 4b), which demonstrated the functionality of the SF/ZnONRs hydrogel as a wearable piezoelectric device. For composite PHs, the effect of piezoelectric filler contents on their piezoelectric performance has been further studied. For instance, Fu et al. investigated the electrical output of PAN-PVDF hydrogels with different PVDF contents.<sup>[75]</sup> As shown in Figure 4c,d, the voltage and current outputs of the hydrogels enhanced as the PVDF content increased from 0 to 20% while decreasing after reaching 20%. Similar results were reported in another PVA/PVDF hydrogel, where the electrical outputs showed opposite trends before and after PVDF content reached 30%.<sup>[87]</sup> Such phenomena occurred due to the high modulus of PVDF ( $\approx 3$  GPa).<sup>[95]</sup> With the introduction of PVDF, those PHs became more rigid, resulting in lower strain under the same mechanical stress, which had a negative impact on their piezo-

electric response. Therefore, a transition point of PVDF content existed with respect to the piezoelectric performance of those PHs. This was also reflected in the variation of their piezoelectric constants, as presented in Figure 4e.

In addition to electrical outputs, other important parameters of the piezoelectric performance of PHs include response time, sensitivity, and durability. Here, the response time refers to the time interval for the voltage output to reach  $\approx 90\%$  of the peak value. Fast response time could significantly enhance the device's ability to promptly detect and respond to external stimuli, making it highly efficient in real-time applications. Sensitivity is usually determined by the voltage output per unit pressure, which can be calculated from the results of voltage-pressure curves. Highly sensitive devices could detect even subtle pressure changes, making them ideal for precision measurements and applications that require high sensitivity and accuracy. Note that sensitivity can be determined through different methods depending on the matrix used by the researchers. Durability represents the ability of the material to generate constant electrical output under long-term cycling tests. Devices demonstrating excellent durability could maintain optimal performance over extended periods of usage, ensuring reliability and longevity in various applications. Taking those parameters into account, PHs are favorable owing to their high flexibility, mechanical stability, and deformability against subtle pressures. For example, a fast-response and highly sensitive nanocomposite PH (Gel/OCS-ABTO) was reported recently.<sup>[91]</sup> As shown in Figure 4f,g, the Gel/OCS-ABTO hydrogel exhibited a rapid response time (24 ms) and an ultrahigh sensitivity ( $49.61 \text{ mV kPa}^{-1}$ ) in the low pressure range. Typically, the voltage-pressure curve of the PH displayed a linear regime and a nonlinear regime (Figure 4g). Within the elastic deformation range of the PH, the voltage increased linearly with pressure while gradually reaching a plateau afterwards due to sharply increased elastic resistance, resulting in a decrease of sensitivity. The durability of the PH was verified by long-term

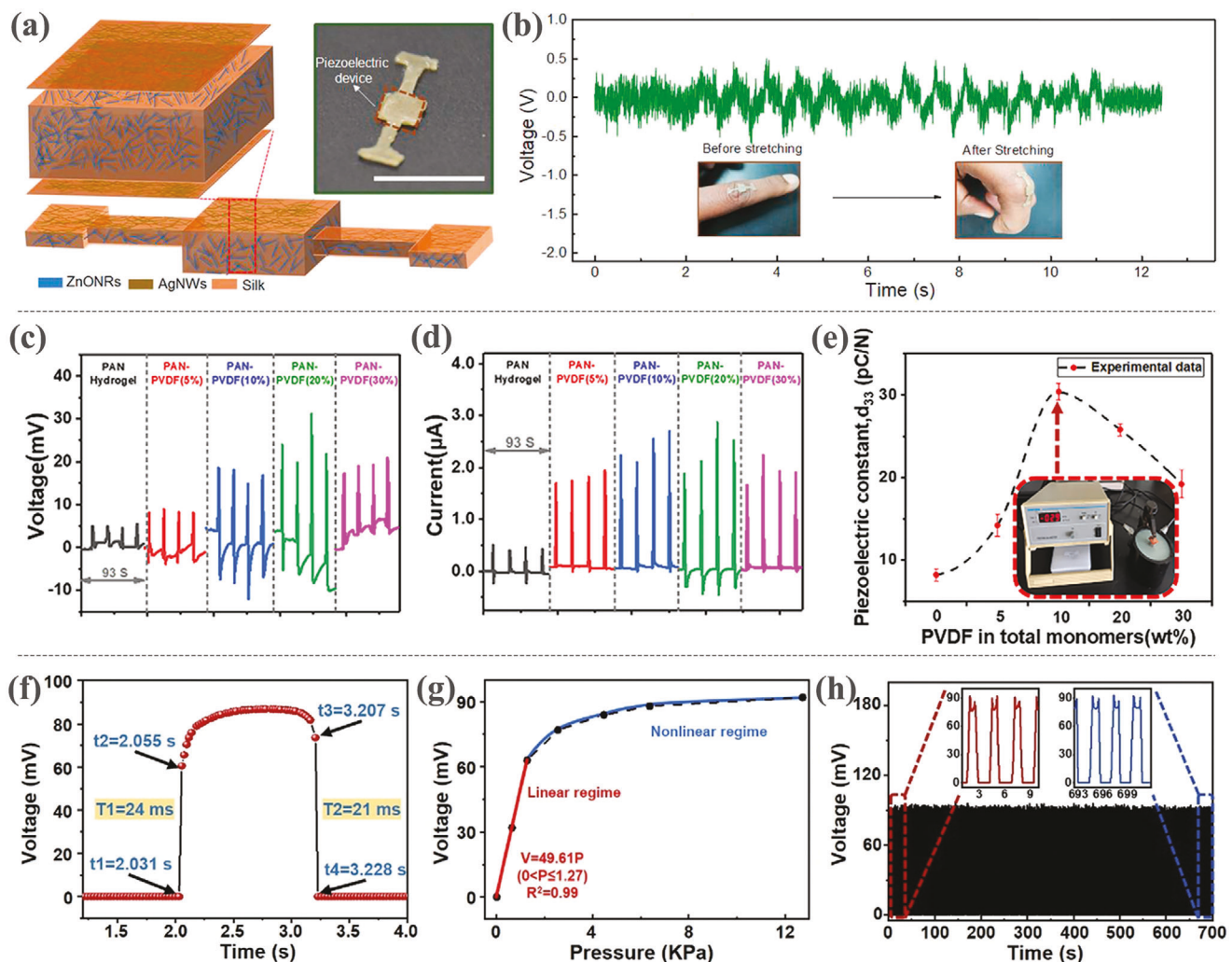


**Figure 4.** Evaluation of the piezoelectric performance of various PH materials. a,b) Piezoelectric response of SF/ZnONRs hydrogels: a) design and digital image of the SF/ZnONRs hydrogel device; b) voltage outputs of the hydrogel device in response to the finger bending and relaxing. Reproduced with permission.<sup>[68]</sup> Copyright 2020, Elsevier. c–e) Piezoelectric performance of PAN-PVDF hydrogels: c) voltage and d) current outputs of the hydrogels with different PVDF content; e) Piezoelectric constant ( $d_{33}$ ) of the hydrogels by varying the PVDF content. Reproduced with permission.<sup>[75]</sup> Copyright 2019, American Chemical Society. f–h) Piezoelectric performance of Gel/OCS-ABTO hydrogels by evaluating: f) response time; g) sensitivity; h) durability. Reproduced with permission.<sup>[91]</sup> Copyright 2023, Elsevier.

operation (>200 times) during which no voltage output attenuation was observed (Figure 4h). The exceptional piezoelectric performance of the reported nanocomposite PH was attributed to its highly interconnected and flexible hydrogel networks with excellent piezoelectric response capability.

The detailed piezoelectric performance of recently reported PHs is summarized in Table 2. In terms of materials, the piezoelectric performance of PHs is significantly determined by the introduced organic piezoelectric polymers or inorganic piezoelectric nanoparticles. In most cases, there is a transition point for the piezoelectric component content, where the best piezoelectric performance of PHs can be obtained. As shown in Table 2, most PHs have a voltage output in the range of tens to hundreds of mV and a current output in the order of nA to  $\mu$ A. It is worth noting that the voltage output of the SF/ZnONRs hydrogel reaches as high as 12.5 V.<sup>[68]</sup> That can be explained by considering that

both ZnONRs and SF  $\beta$ -sheets are capable of generating piezoelectric responses in the PH composite system and meanwhile a positive piezoelectric coupling effect exists between them. In that case, the coupled piezoelectric potential generated by superposed dipole movements would contribute to a significant voltage output. It should also be noted that a high current output of  $\approx 1.6$  mA was obtained by adding polypyrrole (Ppy) into a gelatin/PVDF hydrogel. The introduction of appropriate conductive fillers is beneficial for enhancing the current output of PHs.<sup>[96,97]</sup> Other parameters such as sensitivity, response time, and durability should also be considered according to practical applications. For sensitivity, its unit can be different depending on the characterization methods.<sup>[68,91,93,96]</sup> Furthermore, it is crucial to tune the equilibrium between the piezoelectric performance and the mechanical characteristics of PHs as they often compete and require simultaneous optimization.

**Table 2.** A summary of the piezoelectric performance of recently reported PHs.

| PHs                                     | Voltage          | Current                | Sensitivity                | Response time    | Durability   | Refs. |
|---|------------------|------------------------|----------------------------|------------------|--------------|-------|
| SF/ZnONRs                               | 12.5 V           | 0.04 $\mu$ A           | $\approx$ 320 pC N $^{-1}$ | $\approx$ 50 ms  | >500 cycles  | [68]  |
| Graphene-SF/tannin                      | $\approx$ 5 mV   | —                      | —                          | —                | >21 d        | [98]  |
| PAN-PVDF                                | 18 mV            | 2.2 $\mu$ A            | $\approx$ 30 pC N $^{-1}$  | $\approx$ 31 ms  | >1000 cycles | [75]  |
| PAN/PAM-PVDF                            | $\approx$ 50 mV  | —                      | $\approx$ 3 mV N $^{-1}$   | —                | >300 cycles  | [93]  |
| Gelatin/PVDF/Ppy                        | —                | $\approx$ 1.6 mA       | 32.39 kPa $^{-1}$          | $\approx$ 200 ms | >5000 cycles | [96]  |
| SA/ZnO-PVDF                             | $\approx$ 200 mV | $\approx$ 1.29 $\mu$ A | —                          | —                | —            | [25]  |
| Gel/OCS-ABTO                            | 85–90 mV         | —                      | 49.61 mV kPa $^{-1}$       | 24 ms            | >200 cycles  | [91]  |
| Bacterial cellulose/ ImClO <sub>4</sub> | 140 mV           | —                      | 4 mV kPa $^{-1}$           | —                | >2000 cycles | [72]  |

### 3.2. Flexibility of PHs

Biomedical devices that utilize hydrogels can be either implanted in the human body or maintain intimate contact with the human skin to avoid interference with bodily physiological activities. Consequently, the flexibility of hydrogels is of particular interest within this field to ensure the functionality and long-lasting applicability of these devices while simultaneously providing patient comfort.<sup>[99]</sup> Despite the advantageous properties of pristine hydrogels utilized in biomedically engineered devices, those materials cannot initiate cell regeneration, especially important in wound healing and tissue engineering applications, without an external physical stimulation.<sup>[24,100–102]</sup> Additionally, such devices are mostly powered with external power sources, which have the disadvantage of making the overall device bulky and rigid. Therefore, a solution to address these various issues can be provided by introducing piezoelectricity to the hydrogel. In general, piezoelectric materials are highly versatile and can offer significant functionality across various applications, including the biomedical field.<sup>[28–30]</sup> However, by themselves, they are generally rigid and brittle (200 MPa–200 GPa) compared to the human skin (0.4–0.9 MPa),<sup>[39–43]</sup> and not all piezoelectric materials are biocompatible. To address this issue, piezoelectric materials typically require assimilation with other materials or incorporation of structural designs for acceptable employment in the biomedical field. Thus, the development of PHs would address the disadvantages of both hydrogels and piezoelectric materials, in which the piezoelectric materials serve as the bioelectrical stimulation to initiate cell regenerative processes and the hydrogel matrix preserves the overall device flexibility, all vital considerations that are maintained and even enhanced when utilized in biomedical applications.

PHs derived from natural biopolymers are of great interest due to their inherent flexibility, biocompatibility, and biodegradability. However, most biopolymer hydrogels exhibit brittleness and suffer from poor load-bearing capabilities.<sup>[52,103]</sup> Therefore, achieving excellent flexibility in those natural biopolymer-based PHs remains a challenge. In Zhu et al. and their research, they reported a highly compressible and stretchable SF hydrogel capable of withstanding  $\approx$ 70% compressive strain and  $\approx$ 127% tensile strain, which were enabled by the aforementioned BSICT strategy.<sup>[67]</sup> Ashby plots of the elastic modulus/strain (Figure 5a) and hysteresis/elastic modulus (Figure 5b) show that the developed SF hydrogel is located within the “empty soft material space,” which is a designated almost-empty space for newly developed soft biomaterials with elastic moduli ranging from 1

to 100 MPa.<sup>[104]</sup> The elastic modulus/strain plot (Figure 5a) arranges commonly used biopolymer hydrogels and other soft biomaterials as either elastically stretchable with constrained moduli or rigid with low failure strains, in which their SF hydrogel reached an elastic modulus of  $6.5 \pm 0.2$  MPa. The hysteresis/elastic modulus plot (Figure 5b) classifies the biomaterials based on how effectively they dissipate energy during the loading-unloading cycles, with the SF hydrogel absorbing greater than 60% energy at a strain of 20%. Such remarkable results were attributed to the formation of flexible and robust  $\beta$ -sheets which directly served as physical crosslinks connecting disparate SF chains into continuous networks.

For PHs utilizing synthetic polymers, additional piezoelectric materials are introduced into the hydrogels, which will inevitably affect their mechanical flexibility. Most organic and inorganic piezoelectric materials are relatively rigid or brittle compared to the flexible hydrogel matrix, and the introduction of those materials can affect the crosslinked networks of the hydrogel, which become denser and less homogenous due to physical interactions between the hydrogel polymer chains and the fillers.<sup>[105,106]</sup> Increasing contents of piezoelectric components will correspondingly increase the density and the inhomogeneity of the PH networks, thus leading to decreased mechanical flexibility. Fu et al. investigated the effect of PVDF content on the mechanical behavior of the PAN-PVDF hydrogel.<sup>[75]</sup> Although the tensile strength of the PAN-PVDF hydrogel increased with increasing PVDF content, a significant decrease in its tensile strain was observed (Figure 5c). It was also found that the compressive stress of the hydrogel increased sharply with the compressive strain when the PVDF content reached above 20%, which means a greater force is required to deform the hydrogel, potentially leading to a decrease in its piezoelectric sensitivity. Figure 5d also shows an increase in tensile strength and decrease in elongation at break of the PAN-PVDF hydrogels. This demonstrates a reduction in flexibility as the PVDF content increases. Despite such results, their hydrogels still exhibited low Young's modulus values (1.33–4.24 MPa) comparable to that of the human skin (Figure 5e). Wang et al. reported a PVA/PVDF hydrogel where a decrease in stretchability was observed with an increasing PVDF content.<sup>[87]</sup> Those reported results are consistent with the general case of a composite hydrogel system, where structural inhomogeneity occurs due to the inclusion of additional fillers. However, inconsistent behavior was observed in a recently reported nanocomposite PH (Gel/OCS-ABTO), where overall enhanced flexibility was observed by introducing functionalized BTO nanoparticles into a

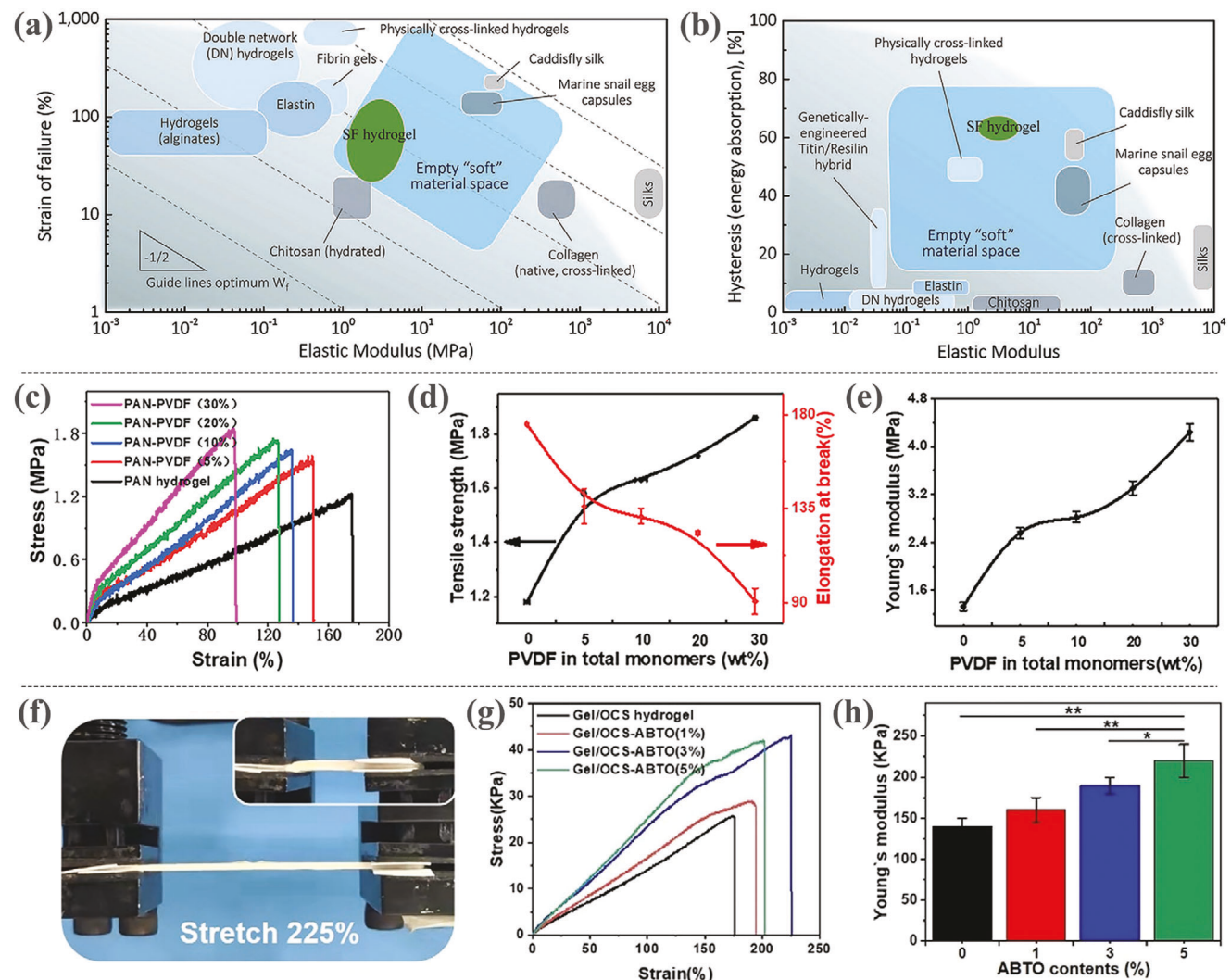


**Figure 5.** Evaluation of the mechanical performance of various PH materials. a,b) Ashby plots of various soft biomaterials: a) elastic modulus/strain; b) hysteresis/elastic modulus. Reproduced with permission.<sup>[67]</sup> Copyright 2018, Wiley. c–e) Mechanical performance of PAN/PVDF hydrogels: c) stress-strain curves; d) tensile strength and elongation curves; e) Young's modulus of the hydrogels with various PVDF concentrations. Reproduced with permission.<sup>[75]</sup> Copyright 2019, American Chemical Society. f–h) Mechanical performance of Gel/OCS-ABTO hydrogels: f) digital image demonstrating the 225% stretchability; g) stress–strain curves and h) Young's modulus of the hydrogels with various ABTO concentrations. Reproduced with permission.<sup>[91]</sup> Copyright 2020, Elsevier.

Gel/OCS hydrogel.<sup>[91]</sup> In contrast to the typical behavior, introducing the BTO nanoparticles actually increased the stretchability of the hydrogel, with the highest strain of 225% obtained at 3% BTO content (Figure 5f). At further increased BTO content, the tensile strain started to decrease since the composite prepolymerized liquid was too viscous and potentially led to fewer areas that contributed in crosslinking (Figure 5g). Although the Young's modulus of the hydrogels also increased with BTO contents, it still remained at low levels (<250 kPa) (Figure 5h). In their work, introducing ABTO nanoparticles not only established a piezoelectric response but also acted as partial crosslinking sites to enhance the flexibility of the hydrogel.

The key mechanical performance of PHs, including their tensile/compressive strength, tensile/compressive strain, and Young's modulus, are summarized in Table 3. The hydrogel

matrix predominantly influences the mechanical characteristics of PHs. Overall, the reported PHs based on both natural biopolymers and synthetic polymers exhibit stretchability or compressibility with low Young's modulus values in the soft and flexible material range (kPa–MPa),<sup>[107]</sup> ensuring applicability in the biomedical field. Nevertheless, significant differences in their flexibility can still be observed by comparing specific tensile/compressive strength and strain. Typically, PHs developed from synthetic polymer hydrogels are able to withstand higher tensile or compressive strain with higher tensile or compressive strength compared to those based on natural biopolymer hydrogels, indicating higher flexibility. This can be explained by the fact that synthetic polymer hydrogels usually have more crosslinking sites and higher gelation strength than that of natural biopolymer hydrogels. Moreover, crosslinking networks also play a

**Table 3.** A summary of the mechanical performance of PHs.

| Hydrogel matrix     | PHs          | Tensile/compressive strength | Tensile/compressive strain | Young's modulus | Refs. |
|---------------------|--------------|------------------------------|----------------------------|-----------------|-------|
| Natural biopolymers | SF           | ≈0.56 MPa/≈1.6 MPa           | ≈127%/≈70%                 | ≈2.6 MPa        | [67]  |
|                     | SF/ZnONRs    | 6.6 kPa/-                    | 28%/-                      | —               | [68]  |
|                     | Gel/OCS-ABTO | 43 kPa/≈200 kPa              | 225%/80%                   | ≈190 kPa        | [91]  |
|                     | Collagen     | -/≈210 kPa                   | -/≈80%                     | ≈960 kPa        | [108] |
| Synthetic polymers  | SA/ZnO-PVDF  | ≈1.4 MPa/-                   | ≈33%/-                     | —               | [25]  |
|                     | PAN-PVDF     | ≈1.63 MPa/≈3 MPa             | ≈131.4%/≈90%               | ≈2.82 MPa       | [75]  |
|                     | PVA-PVDF     | 6.29 MPa/-                   | 300.88%/-                  | 6.4 MPa         | [87]  |
|                     | PAN/PAM-PVDF | ≈1.5 MPa/≈27.5 MPa           | ≈380%/≈90%                 | ≈0.48 MPa       | [93]  |

significant role in the flexibility performance of PHs. By comparing the PAN-PVDF hydrogel with the PAN/PAM-PVDF hydrogel, the latter can withstand almost threefold higher tensile strain while showing even lower Young's modulus. The significant increase in tensile strain is due to the formation of highly ductile and robust double networks resulting in enhanced stretchability of the hydrogel. Meanwhile, the integration of soft PAM chains with relatively rigid PAN chains also contributes to a decrease in Young's modulus, indicating higher flexibility. Therefore, to improve the flexibility of PHs, further efforts can be made in developing multiple-crosslinking PHs or introducing other interactions between polymer chains.

### 3.3. Biocompatibility of PHs

Wearable PH devices intimately interact with the human skin in order to obtain accurate and robust signals. PH devices can also be implanted to promote restoration of human cells such as wound healing or tissue regeneration. Hence, biocompatibility is a significant and essential consideration of PH devices to guarantee a safe user experience and the continuous good health of the users, especially for biomedical applications that involve long-term sensing or monitoring when placed on the skin or implanted within the human body.<sup>[102,109,110]</sup> To verify the biocompatible status of devices used in biomedical engineering applications, evaluation of the given material's cytotoxicity or the level of bioactivity must be achieved,<sup>[111]</sup> and tests demonstrating cell growth and adhesion (Figure 6a,b), cell viability (Figure 6c), and cell migration (Figure 6d,e) can be performed.<sup>[25,87,112,113]</sup> For example, Liang et al. modified ZnO nanoparticles with the PVDF/SA piezoelectric hydrogel scaffold (ZPFSA) using 3D printing technology to accelerate wound healing and minimize scar formation.<sup>[25]</sup> The piezoelectric response is considered the bioelectrical stimulation, which can trigger the proliferation and migration of cells, deposition of ordered collagen, neovascularization and upregulated expression of a multitude of growth factors that facilitate wound healing and more. Here, they verified the biocompatibility and biosafe status of their ZPFSA scaffold through cell growth, adhesion, and viability testing. As shown in Figure 6a, live staining of the L929 cells is shown to demonstrate cell growth, with the fibroblast numbers increasing with coculture time from days 1 to 7. Additionally, despite modifying PVDF with SA and ZnO nanoparticles, fibroblast adhesion and prolif-

eration showed favorable results (Figure 6b). When compared to the control and SA groups, the ZPFSA piezoelectric hydrogel scaffold demonstrated cell morphology that was more comparable to regular fibroblasts, and the activity of cell proliferation was more evident than the other groups. To further confirm the biocompatibility of their composite hydrogel, they conducted a tetrazolium assay (MTT) test, which is considered the gold standard to determine cell viability and proliferation.<sup>[114]</sup> They also achieved cell viability of the two piezoelectric hydrogel scaffold groups of over 90% to verify excellent biocompatibility of their ZPFSA devices (Figure 6c). Serra-Gómez et al. also performed a MTT test using the fibroblast cell line NIH3T3 to confirm biocompatibility of their nanocomposite PH based on a poloxamine gel matrix (Tetronic T1107) and cyclodextrin (CD), which are materials often used in tissue engineering,<sup>[115,116]</sup> and modified them with piezoelectric barium titanate (BT) nanoparticles.<sup>[117]</sup> Given that they incorporated biosafe BT nanoparticles as the piezoelectric material,<sup>[118]</sup> the cell viability test resulted in above 90% viability at low concentrations of poloxamine (<1 wt%) for both pristine T1107 and the composite PH, and a 70 to 90% viability at higher concentrations of poloxamine (1 to 25 wt%). In another case, Wang et al. reported a self-powered PVA/PVDF composite hydrogel, in which strong hydrogen bonds between the PVA and PVDF molecules improved the piezoelectric mechanical properties.<sup>[87]</sup> To demonstrate the level of bioactivity, they observed the migration of L929 cells using an in vitro wound healing assay (Figure 6d), in which the cell migration rate was the quickest for their PVA/PVDF composite hydrogel with the cell-free area having decreased to 9.49% of the original area (Figure 6e). For Xu et al.'s work, they reported an antibacterial PH composite using carboxymethyl chitosan, tannic acid, carbomer, and iron tungstate ( $\text{FeWO}_4$ ) to design wound dressings that exhibit antibacterial efficiency and prevent wound infection. For a comprehensive evaluation of the biocompatibility of their PH composite, they conducted multiple tests to assess its hemocompatibility and cytocompatibility, such as an in vitro hemolysis test, a cell viability test, and live/dead cell staining assay test.<sup>[119]</sup> Hemocompatibility is a good measure of success of in vivo applicability for blood-contacting biomaterials,<sup>[120]</sup> and the hemolysis test for their composite PH displayed good hemocompatibility, with no signs of obvious hemolysis and a very low hemolysis ratio (<5%) when compared to the results of the control group. Furthermore, the cell viability test involved a direct contact test between the hydrogels and L929 cells, with no significant difference noted in cell viability between the two groups. In addition,

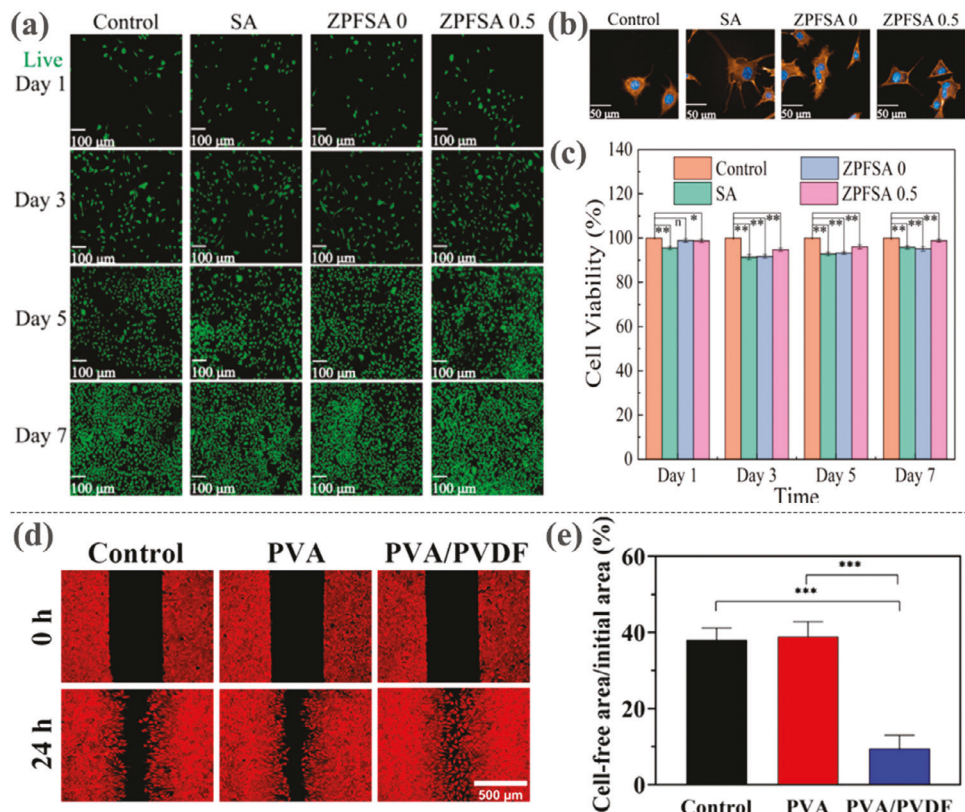


**Figure 6.** The biocompatibility of various PH composite materials. a–c) Biocompatibility evaluation of ZPFSA scaffolds: a) live and dead cell staining; b) fluorescent imaging demonstrating fibroblast adhesion and proliferation; c) cell viability of L929 cells on various ZPFSA scaffolds. Reproduced with permission.<sup>[25]</sup> Copyright 2022, American Chemical Society. d,e) Biocompatibility evaluation of PVA/PVDF scaffolds: d) in vitro healing showing cell migration of the L929 cells after 24 h removal of the culture; e) percentages of cell-free areas after cell migration of the L929 cells of various PVA/PVDF scaffolds. Reproduced with permission.<sup>[87]</sup> Copyright 2022, American Chemical Society.

the live/dead cell staining assay test resulted in no obvious dead cells.

Natural biopolymers such as SF, collagen, and cellulose have inherent high biocompatibility;<sup>[102]</sup> however, synthetic crosslinkers and initiators could be used during the process of polymerization, and much like synthetic composite hydrogels, raise concerns of toxicity.<sup>[19]</sup> Specifically for PHs, they are characterized by their physicochemical properties that regulate protein and cell interfaces under specific temperature, pH, and ionic strength conditions in a miscellaneous biological environment.<sup>[121,122]</sup> This enforces the behavior of the PH onto the organic material with which it comes into intimate contact. On a surface structural level, the outer atomic layer of the material functions as a type of biological transmitter between the cells and the given material, and due to the physicochemical properties, the PHs can molecularly and cellularly change transmission paths to affect material biocompatibility. Moreover, since hydrogel properties such as cell adhesion and differentiation are remarkably similar to that of the ECM, the use of hydrogels within the field of biomedical engineering aids in cell attachment and migration. The cells' biochemical nature is still maintained, which allows for facile nutrient diffusion and transportation while simultaneously providing mechanical and biological support.<sup>[18,123,124]</sup> Due to the hydrophilic nature of hydrogels, cell growth is greatly supported

as it can provide stability and swelling for soft tissues and also form hydrated structures and channels.<sup>[20,124]</sup> Overall, validating the biocompatibility status of PHs is vitally important and a significant part of research regarding biomedical applications as it guarantees the user's safety and continuous good health, especially in cases where long-term usage can be applicable. For PH devices to intimately and safely interact on and inside the human body, they should employ biocompatible and biosafe materials and administer biocompatibility tests that validate their biocompatible status by passing cytotoxicity tests and gauging the level of intended bioactivity.<sup>[19,111]</sup> Failure to meet these biocompatibility standards can potentially result in irreversible damage or scarring to tissues in close contact with PH devices.

### 3.4. Biodegradability of PHs

For wearable and implantable applications of bioelectronic PH devices, assessing and confirming their biocompatibility is important. Particularly in the field of biomedical engineering, when dealing with PH devices that are implantable or maintain intimate and prolonged contact with the human skin, an additional critical factor alongside biocompatibility is the biodegradability of the materials. This ensures the sustained well-being of the

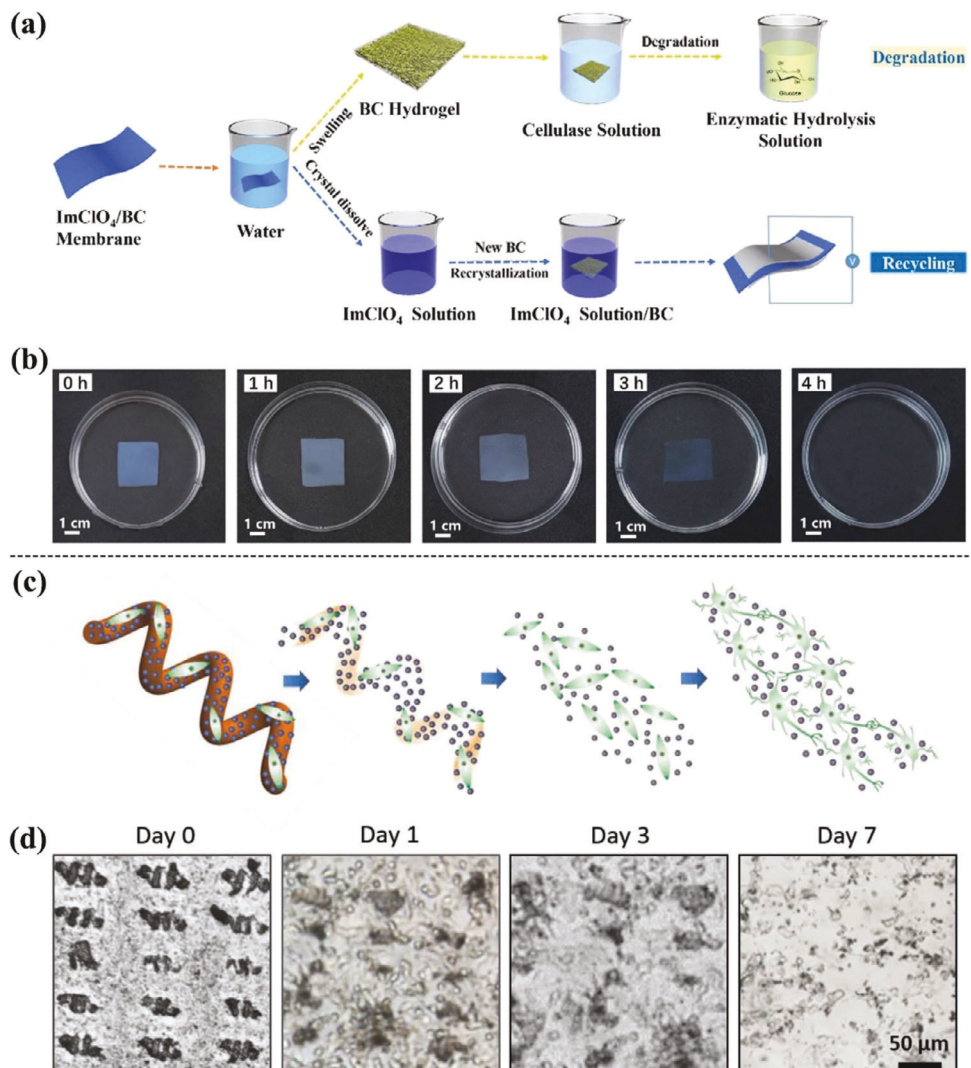


**Figure 7.** The biodegradability of various PH composite materials. a,b) Biodegradability evaluation of the self-powered mechanical sensor consisting of a matrix of BC hydrogel and  $\text{ImClO}_4$ : a) schematic illustration of the biodegradability and recyclability; b) Digital image showing the fully degradable process after 4 h. Reproduced with permission.<sup>[72]</sup> Copyright 2022, American Chemical Society. c,d) Biodegradability evaluation of the SH-SYSY magnetoelectric microswimmers: c) schematic of the degradation process and induced neuronal differentiation through magnetic stimulation; d) digital image of the degradation process after culturing of the cells for 0, 1, 3, and 7 d. Reproduced with permission.<sup>[128]</sup> Copyright 2020, Wiley.

individual, particularly in short-term applications. This significance is emphasized by studies.<sup>[60,101,110]</sup>

For PH devices, soft and natural materials that are biodegradable should be utilized to ensure the continuous comfort of the user and the working biodegradable mechanism within the human body. For example, Lu et al. designed a hybrid PH sensor using bacterial cellulose (BC) hydrogel as the matrix and imidazolium perchlorate ( $\text{ImClO}_4$ ) molecular ferroelectric as the functional ferroelectric metamaterial that exhibits piezoelectric properties.<sup>[72,125,126]</sup> To realize the biodegradability and also the recyclability of the composite material, they infused the molecular ferroelectric, which is a polar molecule that has both inorganic atomic frameworks and organic molecular groups, into the BC matrix.<sup>[127]</sup> As shown in Figure 7a, the composite material breaks down after being immersed in pure water to demonstrate the biodegradability of the BC hydrogel and the recycla-

bility of the  $\text{ImClO}_4$  molecular ferroelectric. For the  $\text{ImClO}_4$ , it dissolved in the water to form a solution with imidazolium and perchlorate ions, and energy-dispersive spectroscopy (EDS) mappings verify that the main elements of the molecular ferroelectric, the N and Cl elements, completely vanished from the composite material. The BC membrane was then immersed in cellulase solution, in which it became fully transparent after 4 h to demonstrate full decomposition of the hydrogel (Figure 7b). Another example is Dong et al.'s fabrication of a soft helical microswimmer using gelatin-methacryloyl (GelMA)-based hydrogel and multiferroic nanoparticles (MENPs) for targeted cell therapy applications specializing in traumatic injuries and diseases regarding the central nervous system.<sup>[128]</sup> Specifically for the ferroelectric nanoparticles, which maintain a core–shell design, they are composed of a  $\text{BiFeO}_3$  (BFO) shell that encapsulates a  $\text{CoFe}_2\text{O}_4$  (CFO) core. After delivery of the cells to the targeted

area, the secretion of proteinases of the surrounding cells degraded the helical structure of the microswimmers, which consisted of the GelMA hydrogel (Figure 7c). The therapeutic cells and the MENPs were then released, and an alternating magnetic field was simultaneously applied to induce the neuronal cell differentiation of the human neuroblastoma SH-SY5Y cell line, which is commonly used for neurodegenerative disease studies. The cell differentiation was caused by the momentary change to the surface charges of the MENPs, which occurred when the CFO cores experienced a strain due to the applied magnetic fields to subsequently exert a strain onto the BFO shells as well. The biodegradable mechanism is verified with optical microscope images of the hybrid microswimmers cultured with SH-SY5Y cells (Figure 7d), in which the helical hydrogel structure gradually biodegrades by day 7. Additionally, Dumitrescu et al. synthesized hydroxyapatite (HA), chitosan, and the piezoelectric smart biomaterial potassium-sodium niobate (KNN) together to develop a PH composite for bone grafting in the field of dentistry.<sup>[129]</sup> To observe in vivo biodegradability of chitosan, which is a natural biodegradable polymer,<sup>[130]</sup> they studied it in simulated physiological fluid substitute medium conditions, which resulted in sufficient degradation of chitosan such that the HA and KNN granules became exposed within the hydrogel composite matrix.

Much like the material biocompatibility of PHs, the level of biodegradability of PHs is also a significant factor for use in biomedical engineering applications, especially when employed in close contact or within the human body. Essentially, the hydrogel biodegradability is determined by the capability of breaking down the crosslinked 3D structures into simple biocompatible products through the process of solubilization, chemical hydrolysis, enzymatic hydrolysis, and more to result in the loss of material integrity.<sup>[19,131]</sup> The four major stages of hydrogel biodegradability are as such: hydration, loss of strength, loss of mass integrity, and loss of mass.<sup>[131]</sup> Some factors that affect the stages of PH biodegradability are molecular weight, level of crystallinity, and polymer hydrophobicity while the pH of the biological environment, concentration of enzymes, and the water quantity affect the rate of biodegradability.<sup>[19]</sup> Specifically, the hydration of the PHs is determined by the polymer hydrophobicity, in which the van der Waals forces and hydrogen bonds of the material must be overcome to destabilize the secondary and tertiary hydrogel structures, resulting in hydration. Loss of polymer strength and loss of mass subsequently occur as the interaction of polymer chains is overcome and crosslinkers are separated. Ultimately, biodegradable PHs have advantages within biomedical applications since they can biodegrade and thus eliminate the need for device removal after an effective yet temporary life span. Thus, the biodegradability of PHs should be evaluated and confirmed to ensure the non-toxicity of the materials and the well-being of the user, particularly when used for applications in health monitoring and restorative purposes.

#### 4. Applications of Piezoelectric Hydrogels in Biomedical Field

Hydrogels are ideal candidates in the biomedical field due to their favorable high flexibility, inherent biocompatibility, and close resemblance to the ECM. In addition to these promising properties,

PHs demonstrate remarkable piezoelectric performance by integrating piezoelectric components, which significantly expands their applications in the field of biomedical engineering. As self-powered devices due to the piezoelectric effect, PHs are able to generate electrical signals under mechanical stress for monitoring purposes and provide variable bioelectric stimulation for facilitation of wound healing and tissue regeneration. Certain PHs derived from natural biopolymers are even capable of biodegradation and show great advantages as implantable devices. Furthermore, leveraging the piezoelectric effect for piezocatalysis opens up the applications of PHs in piezocatalytic medicine. In this section, we review recent advances of PHs in biomedical applications including wound healing and tissue regeneration, piezocatalytic medicine, and health and motion monitoring.

##### 4.1. Wound Healing and Tissue Regeneration

With various advantageous properties such as swelling, self-healing, and stimuli responsiveness, hydrogels have shown immense progress within the biomedical engineering field for cell-culture, tissue regeneration, and drug delivery applications.<sup>[16,20,24,132,133]</sup> However, pristine hydrogels cannot solely activate the process of cell regeneration, which is a crucial component in biomedical restorative applications, and thus require a separate physical stimulation such as light or electrical stimulus to initiate the process.<sup>[24,100]</sup> Moving beyond biomedical devices that incorporate traditional hydrogels, devices that utilize hydrogels endowed with piezoelectric properties have the additional benefit of providing bioelectrical stimulation through the generation of electric polarization under applied mechanical stress. With the ability to generate electrical signals in a localized area, these PH devices can be self-powered. Moreover, they have the potential to facilitate cell regeneration, proliferation and differentiation during tissue growth. This, in turn, promotes processes like re-epithelialization and collagen deposition, blood vessel formation, and an increased secretion rate of growth factors. These effects are observed when the devices maintain intimate contact with the human skin or are implanted within the human body.<sup>[87,102,134]</sup> Such hybrid materials are thus desirable in the design of biomedical devices used for restorative applications in not only tissue regeneration but also wound healing.

Wound healing is a restorative process that involves cell proliferation and migration to facilitate the regeneration of tissues at the site of damage.<sup>[26,27,87,135,136]</sup> Such cell behavior is determined by the endogenous bioelectricity, which can be mimicked by PH devices to facilitate the healing process.<sup>[27,87,136]</sup> For example, Wang et al. designed a PVA/PVDF composite hydrogel for the wound repair of diabetic patients. In this work, the hydrogel provided a moist environment to facilitate the extraction of wound exudate and the PVDF provided electrical stimulation to activate the AKT and ERK1/2 signaling pathways. These pathways are heavily associated with tissue repair and wound healing.<sup>[87,137–139]</sup> With uniform distribution of the PVDF within the PVA matrix, a  $d_{33}$  value of  $8.4 \text{ pC N}^{-1}$  was achieved to generate reported signal outputs of  $2.82 \text{ V}$  and  $248.16 \text{ nA}$ . To verify the wound healing properties of their composite PH dressing, they placed the dressing over the wounds of diabetic rats (Figure 8a)

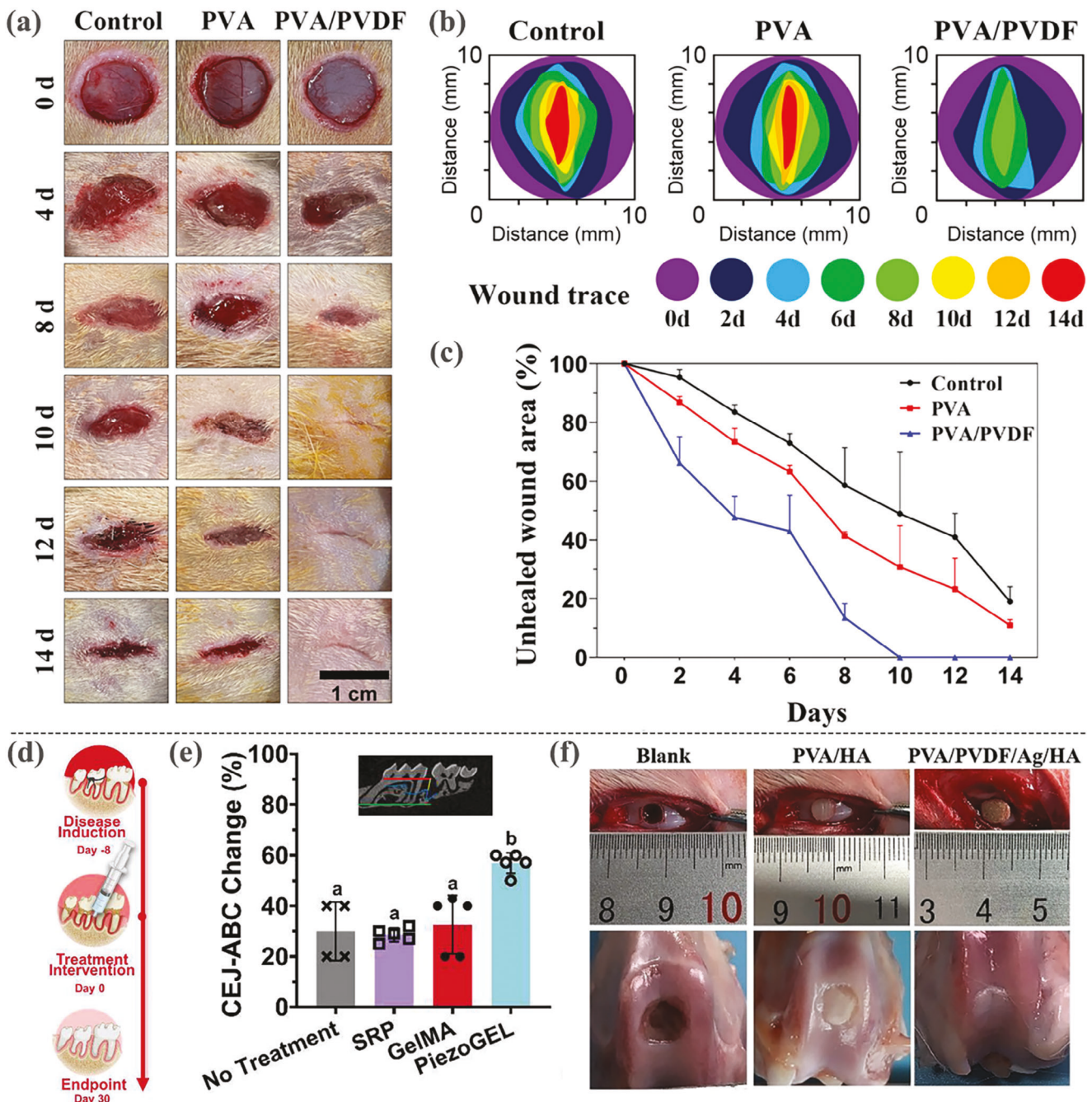


**Figure 8.** PH application in wound healing and tissue regeneration. **a–c)** Wound healing and tissue regeneration evaluation of the PVA/PVDF wound dressing: **a)** digital images of the wound healing process over 14 d; **b)** wound tracking analysis over 14 d; **c)** percentage curves of residual wound area to initial wound area over 14 d when comparing the PH dressing with a pristine PVA dressing and a control group. Reproduced with permission.<sup>[87]</sup> Copyright 2022, American Chemical Society. **d–f)** Wound healing and tissue regeneration evaluation of the GelMA/BTO injectable: **d)** schematic of periodontal disease treatment over the course of 30 d; **e)** graph demonstrating change in cementum–enamel junction; Reproduced with permission.<sup>[140]</sup> Copyright 2023, American Chemical Society. **f)** Digital images of the tissue regeneration process demonstrating osteochondral repair over 12 weeks when comparing the PH injectable with the PVA/HA hydrogel group and a blank group. Reproduced with permission.<sup>[141]</sup> Copyright 2022, MDPI.

and compared the rate of wound healing with that of a control group (untreated) and a pristine PVA dressing. The generation of piezoelectric stimulation from the PH dressing allowed the wound to heal quickly with 13.5% of the initial wound area remaining by day 8 and complete closure by day 10. The accelerated

wound closure rate of the PH dressing was confirmed through wound tracking analysis and demonstrated through a percentage curve of the residual wound area to initial wound area of the three groups (Figure 8b,c). Another example of wound healing is Liang et al.'s SA hydrogel scaffold, modified with ZnO nanoparticles

with PVDF (ZPFSA). This modification aims to provide electrical stimulation through piezoelectricity, promoting wound healing and minimizing scar formation.<sup>[25]</sup> Their PH wound dressing provided a dual piezoelectric release to stimulate vertical swelling and horizontal friction. As a result, stable electric stimulation was provided to the wounded area on rats, in which the wound completely closed within 14 d without any scar tissue formation by utilizing the PH dressing. For wound healing and skin regeneration of wound burns, Chouhan et al. developed a SF-based hydrogel blend through the self-assembly of an equal ratio of two different SFs.<sup>[66]</sup> The fabrication process did not require additional crosslinking agents, which permitted the hydrogel blend to be utilized as an injectable or *in situ* formation for an easy one-step applicability onto third-degree burns. Firm attachment onto the native tissue was noted until the wound completely healed by the 14<sup>th</sup> day, in which they observed wound eschar (dry dead tissue) fall off and the complete regeneration of the neo-epidermis layer.

Similar to wound healing, tissue regeneration is another restorative process that promotes cell proliferation, differentiation, and migration. This regeneration process is often triggered by endogenous bioelectrical stimulation, and one method to provide electrical stimulation is through piezoelectricity.<sup>[27,136,142]</sup> For example, Roldan et al. reported an injectable PH composite using GelMA and biocompatible BTO fillers to promote antibacterial effects and alveolar bone tissue regeneration as a form of periodontal disease treatment.<sup>[143]</sup> Such an oral disease progressively erodes away at the periodontal tissues to ultimately result in teeth loss. However, the use of their PH injectable has reduced inflammation and the pocket depth of the periodontal area after just a month of treatment through the enhancement of early ECM mineralization, bone marrow stem cell (BMSC) viability, and osteogenic differentiation by upregulating osteogenesis-related genes such as RUNX2, COL1A1, and ALP. As shown in Figure 8d, periodontal bone tissue regeneration using the injectable PH composite was evaluated *in vivo* using mice models over the course of 30 d. The change in cementum–enamel junction (Figure 8e) was evaluated to assess the level of tissue regeneration, along with pocket depth of the periodontal area and the change in bone volume at the ligature location. Piezoelectric properties are demonstrated by their PH composite due to the incorporation of piezoelectric BTO fillers, and their PH injectable ultimately provided the highest change of bone tissue and volume regeneration in the periodontal area after a month of treatment when compared to other control groups. Moreover, Wu et al. developed a PVA/PVDF composite doped with silver nanowires (AgNWs) to enhance the piezoelectricity and to evaluate the effect of the piezoelectric performance on osteochondral defect repairs and cartilage formation.<sup>[100]</sup> The function of the piezoelectric response from PVDF was to provide electrical stimulation that would instigate and improve *in vivo* degradation of the materials by activating the enzymes and other degradation mechanisms. By employing their PH composite on the rabbit osteochondral defect model, they successfully demonstrated an enhanced repairing effect of osteochondral defects by mending the cartilage and subchondral bone of the defects (Figure 8f). They observed no evident boundary between the new cartilage and new bone, which meant that the interface between the two was closely attached. Additionally, Li et al. reported a BTO incorporated SF composite PH with integrated piezoelectric prop-

erty, thermal sensitivity, and a storage modulus compared to the natural spinal cord for motor functional recovery of spinal cord injuries.<sup>[92]</sup> The composite PH was directly applied at the lesion site of a rat, where the piezoelectric effect was induced by ultrasound to generate electrical stimulation. It was found that the composite PH significantly enhanced motor function recovery of the spinal cord-injured rats through promoting neurogenesis, axon regrowth, synapse formation, and remyelination. Overall, biomedically engineered devices that employ hydrogels endowed with piezoelectric properties have further applicability in wound healing and tissue regeneration applications. Due to the piezoelectric response of PH composites, electrical stimulation that mimics endogenous bioelectricity is induced to promote cell regeneration, proliferation and differentiation, which are essential to biological restorative processes.

## 4.2. Piezocatalytic Medicine

So far, great efforts have been made in developing innovative and effective treatments for diseases that can meet a wide range of clinical applications. The use of nanomaterials and nanotechnology is widely successful in optimizing therapeutic efficacy and mitigating side effects.<sup>[144,145]</sup> In recent years, the emerging use of piezocatalytic medicine has shown broad application prospects in the biomedical field. The general mechanism of piezocatalysis is based on the ability of piezoelectric materials to release electrons and holes triggered by mechanical energy, which catalyzes the redox reaction of the substrate and generates ROS, including hydroxyl radical ( $\cdot\text{OH}$ ) and superoxide anion ( $\cdot\text{O}_2^-$ ).<sup>[44,45]</sup> As a class of substances with ultra-high reactivity, ROS hold great potential in the field of catalytic medicine, such as cancer therapy and antibacterial therapy.<sup>[46–48]</sup> In contrast to conventional photocatalytic ROS-inducing strategies that have limitations in tissue penetration and controlled regulation, piezocatalysts are able to be controlled by external stimuli to generate ROS without the limitation of penetration depth.<sup>[146,147]</sup> However, piezocatalysts, in terms of piezoelectric nanomaterials, are not fully biocompatible and are usually difficult to deliver to the target location in the body. PHs are desirable to address such issues, since they are highly biocompatible and convenient to deliver while carrying those piezocatalysts. Furthermore, through utilizing different functional hydrogel carriers, PHs can effectively achieve the desired therapeutic environment and be triggered by multiple sources such as ultrasound, thermal, and magnetic stimulation, thus creating the opportunity to combine piezocatalysis with other biomedical technologies.<sup>[148–151]</sup>

As a biocompatible and nontoxic piezoelectric nanomaterial, BTO has attracted much attention in the field of piezocatalytic medicine due to its controllable size, morphology and piezocatalytic activity.<sup>[152–154]</sup> Recently, important progress has been made in the piezocatalytic application of functionalized PHs loaded with BTO. Zhu et al. reported that the piezocatalysis of BTO-loaded PHs triggered by ultrasound can be used for tumor therapy.<sup>[155]</sup> In their work, tetragonal BTO (T-BTO) nanoparticles were synthesized and embedded in a thermosensitive hydrogel to form a composite PH (T-BTO-Gel). The T-BTO-Gel was subsequently injected into the tumor xenografts in mice. As shown in Figure 9a, the piezoelectric effect was triggered by ultrasonic

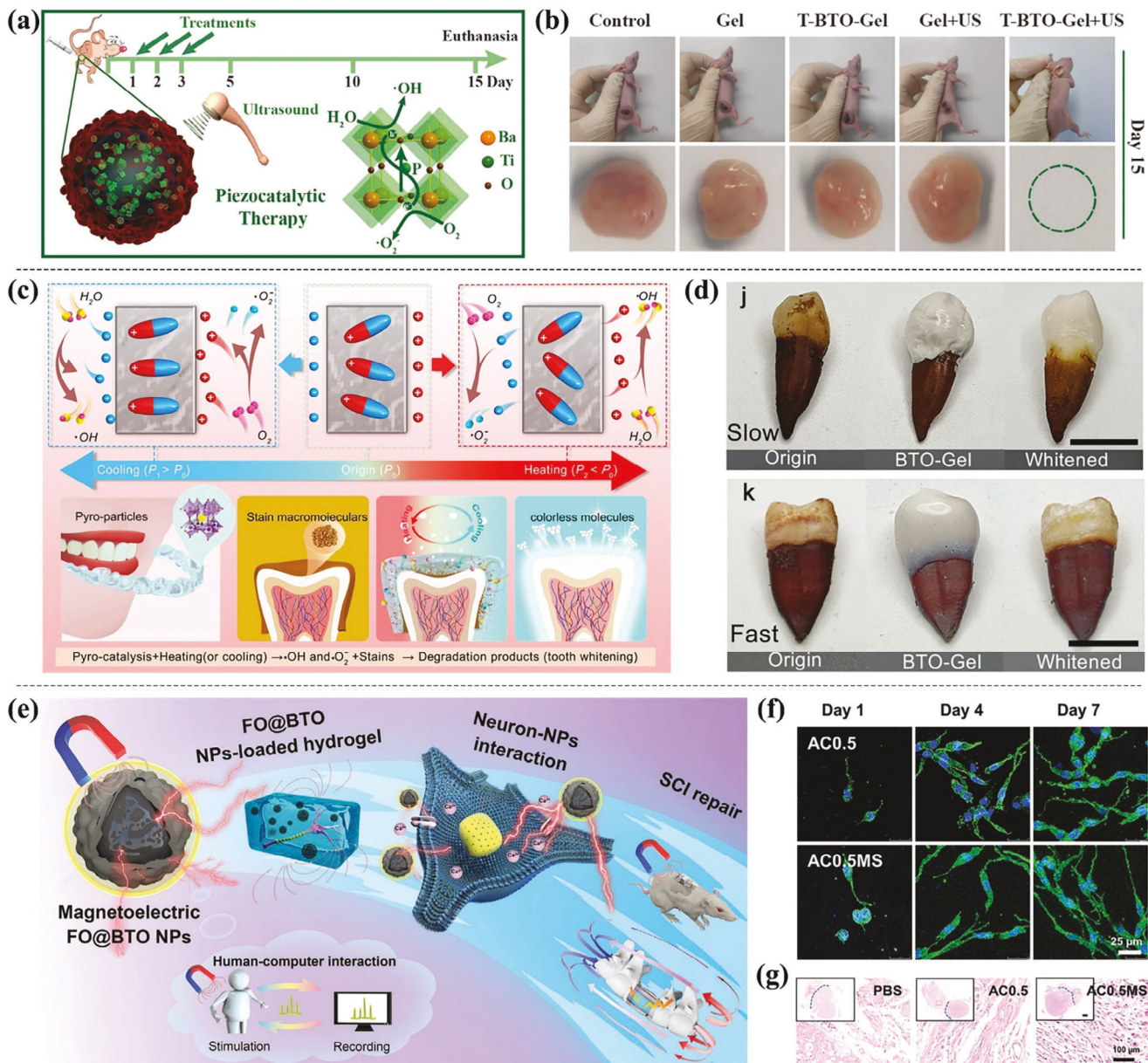


**Figure 9.** Applications of PHs in multi-stimuli triggered piezocatalytic medicine. a,b) Ultrasound triggered piezocatalysis for tumor therapy: a) schematic illustration of piezocatalytic tumor therapy using T-BTO-Gel; b) tumor growth of mice in different comparison groups after 15 d. Reproduced with permission.<sup>[155]</sup> Copyright 2020, Wiley. c,d) Temperature fluctuation induced piezocatalysis for teeth whitening: c) schematic illustration of piezocatalytic teeth whitening via BTO-Gel braces; d) stained tooth before, during, and after whitening at slow and fast heating rate. Reproduced with permission.<sup>[150]</sup> Copyright 2022, Springer Nature. e-g) Application of magnetic field driven piezoelectric effect in nerve injury treatment: e) schematic illustration of piezocatalytic neurogenesis via FO@BTO NPs-loaded hydrogel; f) neural cell proliferation in AC0.5 with and without magnetic stimuli; g) Spin cord cross-sections of mice in different comparison groups 30 d after surgery. Reproduced with permission.<sup>[151]</sup> Copyright 2021, Wiley.

vibration to generate a built-in electric field, leading to the continuous separation and accumulation of electrons and holes, which in turn catalyzed the production of ROS for in situ tumor elimination. After three ultrasound irradiations, the growth of the T-BTO-Gel injected tumor was significantly inhibited and completely eradicated within 15 d, whereas the tumors in the other comparison groups still maintained rapid growth, demonstrating significant therapeutic effect of their designed T-BTO-Gel (Figure 9b). In another work, Wang et al. explored a novel tooth

whitening strategy based on temperature fluctuation-triggered piezocatalysis, which was easily achieved by PHs loaded with BTO nanowires.<sup>[150]</sup> In their research, BTO nanowires were embedded in a photocured hydrogel to form a composite PH (BTO-Gel) with customized shape, which was used as tooth braces. As shown in Figure 9c, heating or cooling led to a polarization alteration in the BTO-Gel, resulting in the release or absorption of screening charges to generate ROS ( $\cdot\text{OH}$  or  $\cdot\text{O}_2^-$ ). The continuously generated ROS attacked and degraded the stains on the

tooth surface, resulting in a tooth whitening effect. Figure 9d shows the results of 2000 thermal cycles of stained teeth at different heating rates with temperature fluctuations of 25 °C. The areas of the teeth covered by BTO-Gel were significantly whiter compared to their initial state, whereas the uncovered areas showed no significant change. Such PH-based piezocatalytic tooth whitening strategy shows great potential for commercialization as it can achieve significant teeth whitening results at a low cost with safety and convenience. In addition, Zhang et al. developed a method to treat nerve injury by triggering PHs through remote magnetic field stimulation.<sup>[151]</sup> Although the mechanism for such neurogenesis is not yet known, it is hypothesized that the generated internal electric field catalyzing the expression of transmembrane ion channels (L-VGCC) and Ca<sup>2+</sup> plays an important role.<sup>[156,157]</sup> Therefore, we include it as additional example of piezocatalytic medicine. As shown in Figure 9e, magneto-responsive ferric oxide (FO) and piezoelectric BTO were prepared into core–shell-structured magnetoelectric nanoparticles (FO@BTO NPs), which were embedded in an aldehyde functionalized-hyaluronic acid/collagen (AHA-Col) hydrogel to form a composite PH. It was found that the AHA-Col hydrogel loaded with 0.5% FO@BTO NPs, denoted as AC0.5, exhibited the best cell viability. Figure 9f shows that neural cells cultured in AC0.5 under a magnetic field are able to spawn more and longer neurites compared to those without magnetic field stimulation, which is attributed to the piezocatalytic effect of AC0.5 triggered by the magnetic field. AC0.5 was implanted into spinal cord-injured rats to validate its *in vivo* therapeutic effects. As shown in Figure 9g, AC0.5 subjected to magnetic field stimulation after 30 d of surgery exhibited significant therapeutic effects compared to other comparison groups, demonstrating the *in vivo* effectiveness of this treatment method.

Here, we introduced various piezocatalytic functions of PHs and their therapeutic roles in diverse medical settings. In brief, the crucial step involves the excitation of the piezoelectric component to form a built-in electric field, leading to the catalysis of a series of redox reactions on the substrate. The high therapeutic efficacy and excellent dynamic responsiveness of such technique make it possible to realize precise, remote, and non-invasive treatments. However, most of the currently studied BTO-based hydrogels are non-biodegradable, potentially posing issues post-implantation. Exploring the piezocatalysis applications using biodegradable PHs is an avenue for future investigation.

#### 4.3. Health and Motion Monitoring

PHs exhibit the characteristics of both hydrogels and piezoelectric materials. On one hand, hydrogels have been widely used as wearable strain sensors for health and motion monitoring due to their high flexibility and biocompatibility to meet ergonomic and safety requirements.<sup>[132,158,159]</sup> Moreover, through various functionalization methods, hydrogels can be endowed with unique properties such as self-adhesion, self-healing, and freezing resistance, enabling wearable hydrogel sensors to detect body signals in various environments.<sup>[132,160]</sup> However, most of those hydrogel sensors are developed based on the piezoresistive mode, which requires an external power source to operate. Despite the flexibility of hydrogel sensors, integrating the necessary power

modules for wearables often leads to a bulky and rigid structure that is not comfortable for wearing and can cause irritability with the skin. On the other hand, piezoelectric materials have shown great advantages in the field of self-powered sensing due to their capability of converting mechanical energy into electrical energy. Currently, most piezoelectric sensors are developed as thin-film devices based on organic or inorganic piezoelectric materials.<sup>[161–165]</sup> Although a lot of advances have been made in piezoelectric thin-film sensors with excellent sensing performance and self-powered capability, their applications in monitoring human body signals are still limited due to their poor biocompatibility and inadequate flexibility. Therefore, PHs combining both hydrogels and piezoelectric materials offer biocompatibility, flexibility, and self-powered capability, exhibiting significant potential for utilization in wearable sensors. These PH sensors can be affixed to diverse locations on the surface of the human body or implanted in the body, enabling real-time monitoring of various physiological signals.

Pulse wave signals are one of the most common and widely studied physiological signals in the human body. They are important indicators of heart rate and vascular aging, which can be detected from the radial artery at the wrist. PHs are favorable in pulse monitoring owing to their flexibility and ability to generate piezoelectric response by subtle pressures. For example, Fu et al. reported the physiological monitoring applications of a piezoelectric PAN-PVDF hydrogel.<sup>[75]</sup> The self-powered PH had a Young's modulus comparable to the human skin and maintained close and safe contact with the wrist for pulse monitoring. As shown in Figure 10a, their PH sensor was able to provide real-time pulse beats with clear distinct signal peaks that allowed for the calculation of the artery augmentation index and the diastolic augmentation index, which diagnosed the level of arterial stiffness. Furthermore, their PH sensor exhibited potential in the detection of vocal cord vibrations. When placed over the Adam's apple of the male volunteer, the PH sensor generated distinguishable electrical signals that corresponded to different words (Figure 10b), which can be used to further open up other approaches in connecting language communication with human behavior. In addition to those physiological signals, PHs can also be used to detect human body signals from various body motions. In a recently reported work, a nanocomposite PH (Gel/OCS-ABTO) that was stretchable, biocompatible, and self-powered was developed for body motion monitoring.<sup>[91]</sup> By grafting the piezoelectric ABTO onto OCS chains within the Gel matrix, the stretchability of the hydrogel was greatly enhanced along with providing the self-powered sensing capability through its piezoelectricity. Monitoring of the elbow flexion and knee flexion was also achieved by wrapping the sensors around the elbow and knee respectively. As shown in Figure 10c, the amplitudes of the output voltage signals notably corresponded to elbow bending angles of 30°, 60°, and 90°. By corresponding knee bending angles with their voltage outputs, knee flexion sensing was also demonstrated for applications involving rehabilitation training (Figure 10d). Their sensor also allowed for foot pressure monitoring involving early detection of conditions and diseases that affect a person's gait, such as diabetes and stroke-related podiatry (Figure 10e). The foot pressure distribution of three scenarios (rear foot on the ground, full foot on the ground, and fore foot on the ground) was monitored, and different pressure distributions on the right foot corresponded to

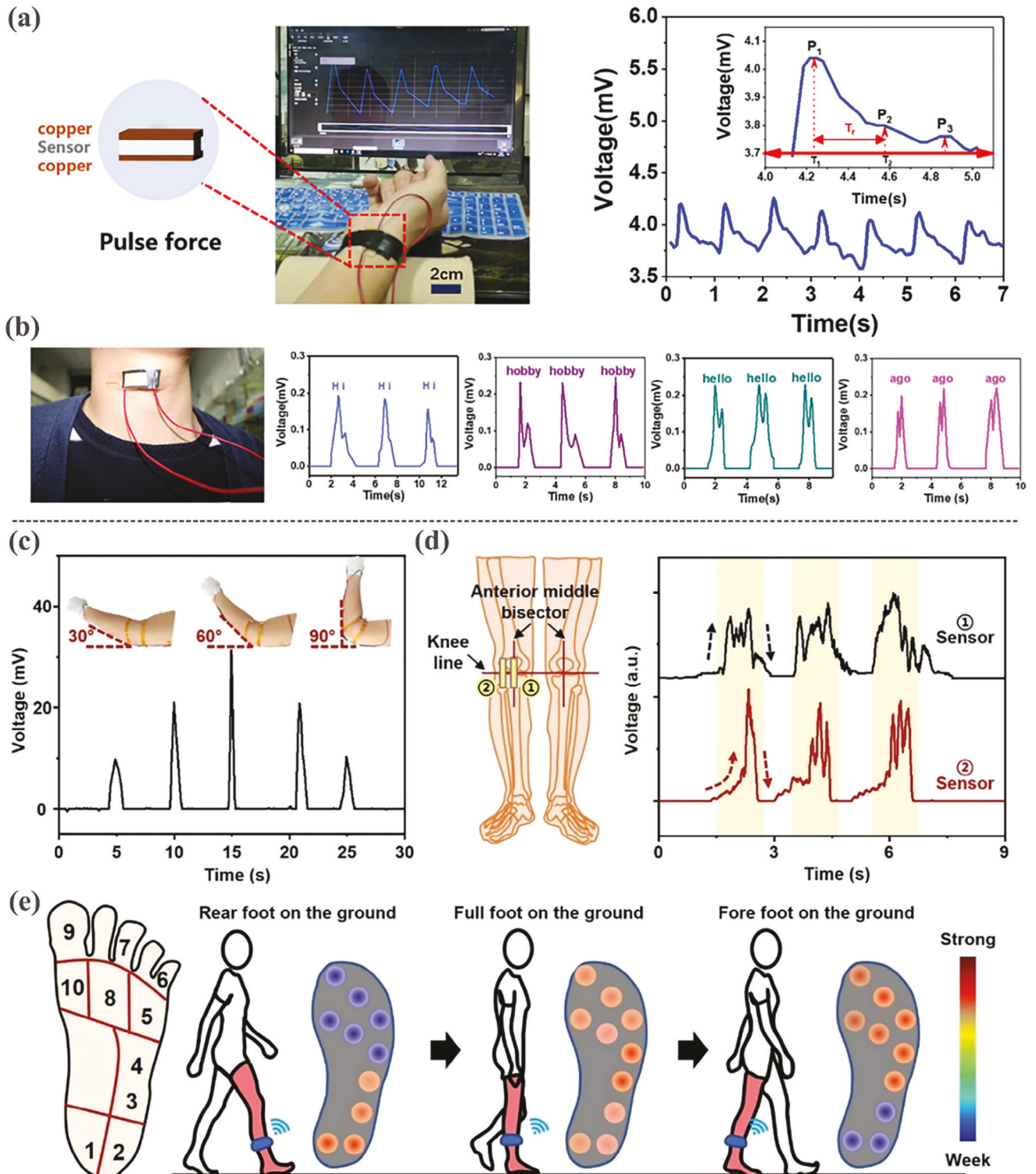


**Figure 10.** Applications of PH devices in health and motion monitoring applications. a) Pulse monitoring and b) vocal cord vibration detection using a PAN-PVDF hydrogel. Reproduced with permission.<sup>[75]</sup> Copyright 2019, American Chemical Society. c) Elbow bending, d) knee flexion, and e) foot pressure monitoring applications of a Gel/OCS-ABTO composite hydrogel. Reproduced with permission.<sup>[91]</sup> Copyright 2023, Elsevier.

**Table 4.** A summary of the biomedical applications of recently reported PHs.

| Biomedical applications      | PHs            | Key properties                                       | Site of action                                  | Stimuli source            | Refs. |
|------------------------------|----------------|--|---|---------------------------|-------|
| Wound healing                | PVA/PVDF       | Piezoelectricity, biocompatibility, flexibility      | Skin wounds of rats                             | Physical activities       | [87]  |
|                              | SA/ZnO-PVDF    | Piezoelectricity, biocompatibility, flexibility      | Skin wounds of rats                             | Physical activities       | [25]  |
|                              | SF             | Piezoelectricity, biocompatibility, biodegradability | Burn wounds of rats                             | Physical activities       | [66]  |
| Tissue regeneration          | GelMA/BTO      | Piezoelectricity, biocompatibility, biodegradability | Periodontal pockets of rats                     | Mastication               | [140] |
|                              | PVA/PVDF       | Piezoelectricity, biocompatibility                   | Osteochondral defects of rabbits                | Mechanical stress         | [141] |
|                              | PAN/PAM-PVDF   | Piezoelectricity, biocompatibility, flexibility      | Human umbilical vein endothelial cells (HUEVCs) | Ultrasound                | [93]  |
| Piezocatalytic medicine      | T-BTO-Gel      | Piezoelectricity, biocompatibility                   | Tumor xenografts of rats                        | Ultrasound                | [155] |
|                              | BTO-Gel        | Piezoelectricity, biocompatibility, biodegradability | Human tooth surface                             | Heating, cooling          | [150] |
|                              | FO@BTO/AHA-Col | Piezoelectricity, biocompatibility, biodegradability | Spinal cord of rats                             | Magnetic field            | [151] |
| Health and motion monitoring | PAN-PVDF       | Piezoelectricity, flexibility                        | Wrist, throat                                   | Pulse beats, vocalization | [75]  |
|                              | Gel/OCS-ABTO   | Piezoelectricity, flexibility                        | Elbow, knee, foot                               | Body motion               | [91]  |
|                              | SF/ZnONRs      | Piezoelectricity, flexibility                        | Chest   | Respiration               | [68]  |

each scenario. For motion monitoring applications of both wearable and implantable PHs, Gogurla et al. incorporated piezoelectric ZnONRs into soft, biocompatible, and conformable SF hydrogel to design a self-powered artificial energy-skin for biophysiological sensing.<sup>[68]</sup> The artificial skin was capable of monitoring finger movements when attached to the finger and the human respiration cycle when attached to the chest through dual transduction mechanisms. As an implantable device, it was embedded into biological tissues and external stimulus of finger pressing was steadily monitored. Overall, not a lot of applications with PHs has been reported yet for health and motion monitoring purposes. Given that the majority of these applications have been published in recent years, there is an expectation that the PH will continue to shine as a rising star in the field of health and motion monitoring.

In this section, we have overviewed recent advances of PHs in biomedical applications, which include common applications such as wound healing and tissue regeneration and health and motion monitoring. Piezocatalytic medicine, an emerging biomedical application, is also detailed to demonstrate the adaptability of the hybrid material system by endowing hydrogels with piezoelectric properties. In **Table 4**, the various biomedical applications of PHs, along with their key properties, site of action, and stimuli source, are cohesively summarized. Overall, piezoelectricity and biocompatibility are considered the key properties of PHs under almost all application scenarios, thus making such hybrid materials desirable within the biomedical field. Specifically, for wound healing and monitoring applications, the flexibility of PHs is also a key property that is mentioned to ensure that they comply with body motions since these devices would be utilized as long-term wearables. For applications in tissue regeneration and piezocatalytic medicine, the biodegradability of PHs is favorable, meaning that no removal surgery is required

after implantation, thus enhancing the convenience of this material. It should also be noted that existing PHs have been utilized at various sites of action, either on the surface of the human skin or implanted within the body, with multiple stimuli sources, which demonstrate wide-ranging applicability regarding the human body and broad development prospects. As such, we envision that future efforts will further explore the potential of PHs in the biomedical field.

## 5. Conclusion and Perspectives

In this review, we summarize and highlight recent advances in PHs with respect to their design strategies, outstanding properties, and applications in the field of biomedical engineering. Overall, a variety of PHs has been developed utilizing natural biopolymer hydrogels or synthetic polymer hydrogels. On one hand, PHs can be directly derived by the physical crosslinking of natural biopolymers with inherent piezoelectricity such as SF, which require no additional chemicals or piezoelectric components to effectively avoid the effects of introducing external materials on the biocompatibility of hydrogels. On the other hand, PHs can also be fabricated in terms of composite hydrogels through integrating diverse synthetic polymer hydrogels with organic or inorganic piezoelectric materials such as PVDF and BTO via physical or chemical interactions, thus revealing great design flexibility and performance tunability. The combination of hydrogels and piezoelectric materials as PHs results in unique gain-of-function with piezoelectricity, flexibility, and biocompatibility. Moreover, the piezoelectric performance of PHs is closely associated with their piezoelectric components. By tailoring the dosage of those piezoelectric components in PHs, high electrical output or sensitivity can be obtained. Meanwhile, attention should also be paid to their durability to ensure long-term use. The

flexibility and biocompatibility of PHs are mainly determined by their hydrogel matrix. In general, PHs utilizing synthetic polymer hydrogels are more flexible and robust than those based on natural biopolymer hydrogels. However, their flexibility may decrease with increased contents of the introduced piezoelectric materials. Therefore, it is important to regulate the usage of those materials to balance their mechanical characteristics and piezoelectric performance. As for biocompatibility, natural biopolymer-based PHs demonstrate apparent superiority due to their inherent biocompatible nature. Moreover, most of them are capable of biodegradation and show great advantages as biomedical devices. All of these promising properties of PHs contribute to their significant potential in biomedical applications including wound healing and tissue regeneration, piezocatalytic medicine, and health and motion monitoring.

Even though remarkable progress has been achieved in PHs for biomedical applications, there are still significant challenges on their way from bench to bedside. From the material perspective, a majority of current efforts are focused on PHs utilizing synthetic polymer hydrogels due to their controllable and facile fabrication. To achieve high piezoelectric performance, piezoelectric components such as PVDF and BTO are usually introduced. However, those piezoelectric materials are not fully biocompatible, and their long-term implant safety is not yet verified. Another concern for synthetic polymer-based PHs is that most of them are non-biodegradable and may pose issues post-implantation. Natural biopolymer-based PHs such as SF hydrogels show excellent biodegradability, but most of them suffer from low piezoelectric potential, which cannot meet the requirements in specific biomedical applications such as tissue regeneration. Although other piezoelectric materials can be incorporated to increase outputs, achieving effective interactions between those materials and biopolymers remains challenging. As a result, the piezoelectric performance of those PHs is usually enhanced at the expense of their mechanical performance. In addition, the intrinsic drawbacks of natural biopolymer-based PHs in customization and complex material processing are yet to be overcome, preventing them from large-scale use in practical applications. Therefore, future efforts should be directed to address these aspects for the development of PHs.

From the application perspective, we put forward specific challenges and future outlook for PHs regarding their biomedical applications. For tissue engineering and piezocatalytic medicine applications, the primary challenge lies in transitioning from animal studies to human applications. Despite the breakthroughs that have been made, most of the existing studies still remain at the animal level. Given that the human body is significantly more complex than the animal body, it is imperative to thoroughly investigate both the effectiveness and potential side effects of PHs on the human body. Another critical challenge is the adaptability of PHs to meet the needs under different biological circumstances. PHs are able to generate electrical stimulation that mimics endogenous bioelectricity within or on the surface of the biological tissue. However, their performance is significantly affected by the stimuli received from those biological tissues, which can vary depending on specific tissues and locations. To further evaluate the *in vivo* effectiveness of PHs, systematic and comprehensive studies need to be carried out regarding various tissues and biological sites. Additionally, the variability across pa-

tients should also be taken into consideration since patient-to-patient variability in weight, gender, age, and other systematic factors can influence responses. Lastly, in order to realize clinical translation of PHs, more attention should be paid to the lifespan, ease of implantation and removal, and their impact on patients. For health and motion monitoring applications, despite their advantage of being self-powered, the functions of PH devices remain limited. Future efforts need to be made toward addressing their multifunctionality. For example, an ideal health-monitoring device should be able to collect multiple physiological signals such as pulse, electrocardiogram, seismocardiogram, electromyogram, and more.

Furthermore, on top of basic properties including mechano-electroresponsiveness, flexibility, and biocompatibility, PH devices should also incorporate functions of data generation, wireless transmission, as well as human-machine interactions. Integration of all these functions into a PH device will undoubtedly require the convergence of interdisciplinary technologies in materials science, biomedical, mechanical, and electrical engineering. Another concern for PH-based monitoring devices is their wearing or implanting convenience for daily activities. For instance, they may be customized into smart bracelets, rings, or even integrated with an existing biomedical device, such as the pacemaker. Further developments of such designs need to leverage technological innovations in product processing and packaging. In addition to aforementioned applications, PHs also exhibit huge potential in biorobots applications.<sup>[166]</sup> Piezoelectric materials have been widely used as actuators due to their reverse piezoelectric effect.<sup>[167–170]</sup> The integration of their actuating features along with flexible and biocompatible hydrogels facilitates the development of biorobots with *in vivo* mobility, which is promising for realizing breakthrough functions such as dynamic drug delivery. Consequently, challenges and opportunities coexist. Despite the limited existing research on PHs, we believe that the broad prospects of PHs in biomedical applications will enable them to enter human life in the near future. As the PH is gaining prominence as a rising star, the exploration of its full potential offers valuable insights into a promising hybrid biomaterial and its potential applications in biomedical applications. This endeavor lays the groundwork for future research, innovation, and the practical utilization of PHs with the goal of advancing healthcare, technology, and the medical world.

## Acknowledgements

The authors acknowledge financial support from the National Science Foundation award (ECCS 2106459, PI: L.D.), the American Heart Association Institutional Research Enhancement Award (23AIREA1048411, PI: L.D.), and the startup fund from the Department of Mechanical and Industrial Engineering at New Jersey Institute of Technology (NJIT).

## Conflict of Interest

The authors declare no conflict of interest.

## Keywords

biomedical applications, hybrid biomaterials, hydrogels, piezoelectric materials

Received: November 6, 2023

Revised: January 12, 2024

Published online:

[1] J. C. Newell, *Biomed. Eng. Online* **2012**, *11*, 94.

[2] R. Agrawal, A. Kumar, M. K. A. Mohammed, S. Singh, *J. Zhejiang Univ., Sci., A* **2023**, *24*, 1027.

[3] S. S. Yousaf, C. Houacine, I. Khan, W. Ahmed, M. J. Jackson, in *Advances in Medical and Surgical Engineering* (Eds: W. Ahmed, D. A. Phoenix, M. J. Jackson, C. P. Charalambous), Academic Press, San Diego, CA, **2020**, pp. 151.

[4] R. Langer, *Chem. Eng. Sci.* **1995**, *50*, 4109.

[5] A. Bharadwaj, *IOP Conf. Ser.: Mater. Sci. Eng.* **2021**, *1116*, 012178.

[6] Y. Mohd, Y. Khan, M. Khan, Yaqub, M.-H. Chen, *Int. J. Bio-Pharma Res.* **2019**, *8*, 2788.

[7] B. D. Ratner, *Annu. Rev. Biomed. Eng.* **2019**, *21*, 171.

[8] C. Kalirajan, A. Dukle, A. J. Nathanael, T. H. Oh, G. Manivasagam, *Polymers* **2021**, *13*, 3015.

[9] M. L. Becker, J. A. Burdick, *Chem. Rev.* **2021**, *121*, 10789.

[10] S. Bhat, A. Kumar, *Biomatter* **2013**, *3*, e24717.

[11] J. Enderle, J. Bronzino, *Introduction to Biomedical Engineering*, Academic Press, San Diego, CA, **2012**.

[12] P. Verdonck, *Advances in Biomedical Engineering*, Elsevier, Amsterdam **2008**.

[13] K. Y. Lee, D. J. Mooney, *Chem. Rev.* **2001**, *101*, 1869.

[14] N. Nieto, M. P. Lutolf, *Syst. Synth. Biol.* **2011**, *5*, 11.

[15] Y. Kim, H. Ko, I. K. Kwon, K. Shin, *Int. Neurorol. J.* **2016**, *20*, S23.

[16] Q. Chai, Y. Jiao, X. Yu, *Gels* **2017**, *3*, 6.

[17] S. K. Kailasa, D. J. Joshi, M. R. Kateshiya, J. R. Koduru, N. I. Malek, *Mater. Today Chem.* **2022**, *23*, 100746.

[18] B. V. Slaughter, S. S. Khurshid, O. Z. Fisher, A. Khademhosseini, N. A. Peppas, *Adv. Mater.* **2009**, *21*, 3307.

[19] N. Das, in *Cellulose-Based Superabsorbent Hydrogels* (Ed: M. I. H. Mondal), Springer International Publishing, Cham, Switzerland, **2019**, p.1433.

[20] E. M. Ahmed, *J. Adv. Res.* **2015**, *6*, 105.

[21] S. Bashir, M. Hina, J. Iqbal, A. H. Rajpar, M. A. Mujtaba, N. A. Alghamdi, S. Wageh, K. Ramesh, S. Ramesh, *Polymers* **2020**, *12*, 2702.

[22] P. Nezhad-Mokhtari, M. Ghorbani, L. Roshangar, J. Soleimani Rad, *Eur. Polym. J.* **2019**, *117*, 64.

[23] J. Siepmann, R. A. Siegel, M. J. Rathbone, *Fundamentals and Applications of Controlled Release Drug Delivery*, Vol. 3, Springer, New York, **2012**.

[24] N. Eslahi, M. Abdorahim, A. Simchi, *Biomacromolecules* **2016**, *17*, 3441.

[25] J. Liang, H. Zeng, L. Qiao, H. Jiang, Q. Ye, Z. Wang, B. Liu, Z. Fan, *ACS Appl. Mater. Interfaces* **2022**, *14*, 30507.

[26] L. Wang, L. Mao, F. Qi, X. Li, M. Wajid Ullah, M. Zhao, Z. Shi, G. Yang, *Chem. Eng. J.* **2021**, *424*, 130563.

[27] G. Thrivikraman, S. K. Boda, B. Basu, *Biomaterials* **2018**, *150*, 60.

[28] M. T. Chorsi, E. J. Curry, H. T. Chorsi, R. Das, J. Baroody, P. K. Purohit, H. Ilies, T. D. Nguyen, *Adv. Mater.* **2019**, *31*, 1802084.

[29] S. Mohammadpourfazeli, S. Arash, A. Ansari, S. Yang, K. Mallick, R. Bagherzadeh, *RSC Adv.* **2023**, *13*, 370.

[30] X. Cao, Y. Xiong, J. Sun, X. Zhu, Q. Sun, Z. L. Wang, *Adv. Funct. Mater.* **2021**, *31*, 2102983.

[31] X. Zhou, G. Xue, H. Luo, C. R. Bowen, D. Zhang, *Prog. Mater. Sci.* **2021**, *122*, 100836.

[32] M. Acosta, N. Novak, V. Rojas, S. Patel, R. Vaish, J. Koruza, G. A. Rossetti Jr, J. Rödel, *Appl. Phys. Rev.* **2017**, *4*, 041305.

[33] T. N. Nguyen, H.-C. Thong, Z.-X. Zhu, J.-K. Nie, Y.-X. Liu, Z. Xu, P.-S. Soon, W. Gong, K. Wang, *J. Mater. Res.* **2021**, *36*, 996.

[34] Q. Zhou, K. H. Lam, H. Zheng, W. Qiu, K. K. Shung, *Prog. Mater. Sci.* **2014**, *66*, 87.

[35] S. Priya, D. J. Inman, *Energy Harvesting Technologies*, Vol. 21, Springer, New York, **2009**.

[36] L. Dong, A. B. Closson, M. Oglesby, D. Escobedo, X. Han, Y. Nie, S. Huang, M. D. Feldman, Z. Chen, J. X. J. Zhang, *Nano Energy* **2019**, *66*, 104085.

[37] L. Dong, X. Han, Z. Xu, A. B. Closson, Y. Liu, C. Wen, X. Liu, G. P. Escobar, M. Oglesby, M. Feldman, Z. Chen, J. X. J. Zhang, *Adv. Mater. Technol.* **2019**, *4*, 1800148.

[38] Z. Lu, C. Zhang, S. H. Kwon, Z. Jiang, L. Dong, *Adv. Mater. Interfaces* **2023**, *10*, 2202173.

[39] M. S. Sukiman, A. Andriyana, B. C. Ang, H. S. C. Metselaar, *Polym. Test.* **2020**, *81*, 106218.

[40] H. S. Kim, D. W. Lee, D. H. Kim, D. S. Kong, J. Choi, M. Lee, G. Murillo, J. H. Jung, *Nanomaterials* **2018**, *8*, 777.

[41] F. Cordero, *J. Appl. Phys.* **2017**, *123*, 094103.

[42] M. Manoharan, A. Desai, G. Neely, A. Haque, *J. Nanomater.* **2008**, *2008*, 849745.

[43] M. Pawlaczek, M. Lelonkiewicz, M. Wieczorowski, *Postepy Dermatol. Alergol.* **2013**, *30*, 302.

[44] M. Wang, B. Wang, F. Huang, Z. Lin, *Angew. Chem., Int. Ed.* **2019**, *58*, 7526.

[45] Y. Feng, L. Ling, Y. Wang, Z. Xu, F. Cao, H. Li, Z. Bian, *Nano Energy* **2017**, *40*, 481.

[46] S. Liang, X. Deng, P. Ma, Z. Cheng, J. Lin, *Adv. Mater.* **2020**, *32*, 2003214.

[47] X. Qian, Y. Zheng, Y. Chen, *Adv. Mater.* **2016**, *28*, 8097.

[48] Z. Tang, Y. Liu, M. He, W. Bu, *Angew. Chem., Int. Ed.* **2019**, *58*, 946.

[49] Y. Zhong, H. Xiao, F. Seidi, Y. Jin, *Biomacromolecules* **2020**, *21*, 2983.

[50] S.-B. Park, E. Lih, K.-S. Park, Y. K. Joung, D. K. Han, *Prog. Polym. Sci.* **2017**, *68*, 77.

[51] B. Balakrishnan, R. Banerjee, *Chem. Rev.* **2011**, *111*, 4453.

[52] D. K. Patel, E. Jung, S. Priya, S.-Y. Won, S. S. Han, *Carbohydr. Polym.* **2024**, *323*, 121408.

[53] B. Tandon, A. Magaz, R. Balint, J. J. Blaker, S. H. Cartmell, *Adv. Drug Delivery Rev.* **2018**, *129*, 148.

[54] J. Liao, H. Huang, *Biomacromolecules* **2020**, *21*, 2574.

[55] X. Tong, W. Pan, T. Su, M. Zhang, W. Dong, X. Qi, *React. Funct. Polym.* **2020**, *148*, 104501.

[56] S. Strassburg, S. Zainuddin, T. Scheibel, *Adv. Energy Mater.* **2021**, *11*, 2100519.

[57] A. Veronica, I. m. Hsing, *ChemPhysChem* **2021**, *22*, 2266.

[58] B. Zhu, H. Wang, W. R. Leow, Y. Cai, X. J. Loh, M.-Y. Han, X. Chen, *Adv. Mater.* **2016**, *28*, 4250.

[59] C. Wang, K. Xia, Y. Zhang, D. L. Kaplan, *Acc. Chem. Res.* **2019**, *52*, 2916.

[60] D.-L. Wen, D.-H. Sun, P. Huang, W. Huang, M. Su, Y. Wang, M.-D. Han, B. Kim, J. Brugger, H.-X. Zhang, X.-S. Zhang, *Microsyst. Nanoeng.* **2021**, *7*, 35.

[61] S. Keten, Z. Xu, B. Ihle, M. J. Buehler, *Nat. Mater.* **2010**, *9*, 359.

[62] T. Yucel, P. Cebe, D. L. Kaplan, *Adv. Funct. Mater.* **2011**, *21*, 779.

[63] Q. Lu, S. Bai, Z. Ding, H. Guo, Z. Shao, H. Zhu, D. L. Kaplan, *Adv. Mater. Interfaces* **2016**, *3*, 1500687.

[64] D. Kuang, F. Jiang, F. Wu, K. Kaur, S. Ghosh, S. C. Kundu, S. Lu, *Int. J. Biol. Macromol.* **2019**, *134*, 838.

[65] S. K. Singh, B. K. Bhunia, N. Bhardwaj, S. Gilotra, B. B. Mandal, *Mol. Pharmaceutics* **2016**, *13*, 4066.

[66] D. Chouhan, T.-u. Lohe, P. K. Samudrala, B. B. Mandal, *Adv. Healthcare Mater.* **2018**, *7*, 1801092.

[67] Z. Zhu, S. Ling, J. Yeo, S. Zhao, L. Tozzi, M. J. Buehler, F. Omenetto, C. Li, D. L. Kaplan, *Adv. Funct. Mater.* **2018**, *28*, 1704757.

[68] N. Gogurla, B. Roy, S. Kim, *Nano Energy* **2020**, *77*, 105242.

[69] X. Yang, J. Liu, Y. Pei, X. Zheng, K. Tang, *Energy Environ. Mater.* **2020**, *3*, 492.

[70] H. Li, M. Long, H. Su, L. Tan, X. Shi, Y. Du, Y. Luo, H. Deng, *Carbo-hydr. Polym.* **2022**, *290*, 119482.

[71] M. Nair, Y. Calahorra, S. Kar-Narayan, S. M. Best, R. E. Cameron, *Nanoscale* **2019**, *11*, 15120.

[72] J. Lu, S. Hu, W. Li, X. Wang, X. Mo, X. Gong, H. Liu, W. Luo, W. Dong, C. Sima, Y. Wang, G. Yang, J.-T. Luo, S. Jiang, Z. Shi, G. Zhang, *ACS Nano* **2022**, *16*, 3744.

[73] M. Irimia-Vladu, E. D. Głowacki, G. Voss, S. Bauer, N. S. Sariciftci, *Mater. Today* **2012**, *15*, 340.

[74] X. Hu, K. Shmelev, L. Sun, E.-S. Gil, S.-H. Park, P. Cebe, D. L. Kaplan, *Biomacromolecules* **2011**, *12*, 1686.

[75] R. Fu, L. Tu, Y. Zhou, L. Fan, F. Zhang, Z. Wang, J. Xing, D. Chen, C. Deng, G. Tan, P. Yu, L. Zhou, C. Ning, *Chem. Mater.* **2019**, *31*, 9850.

[76] Z. Wang, Z. Liu, G. Zhao, Z. Zhang, X. Zhao, X. Wan, Y. Zhang, Z. L. Wang, L. Li, *ACS Nano* **2022**, *16*, 1661.

[77] D. Huang, Y. Cheng, G. Chen, Y. Zhao, *Research* **2023**, *6*, 00022.

[78] E. M. Ahmed, *J. Adv. Res.* **2015**, *6*, 105.

[79] U. S. K. Madduma-Bandarage, S. V. Madihally, *J. Appl. Polym. Sci.* **2021**, *138*, 50376.

[80] P. Lavrador, M. R. Esteves, V. M. Gaspar, J. F. Mano, *Adv. Funct. Mater.* **2021**, *31*, 2005941.

[81] F.-L. Yi, F.-L. Guo, Y.-Q. Li, D.-Y. Wang, P. Huang, S.-Y. Fu, *ACS Appl. Mater. Interfaces* **2021**, *13*, 32084.

[82] H. Jung, M. K. Kim, J. Y. Lee, S. W. Choi, J. Kim, *Adv. Funct. Mater.* **2020**, *30*, 2004407.

[83] R. Fu, L. Tu, Y. Guan, Z. Wang, C. Deng, P. Yu, G. Tan, C. Ning, L. Zhou, *Nano Energy* **2022**, *103*, 107784.

[84] W. Shi, Z. Wang, H. Song, Y. Chang, W. Hou, Y. Li, G. Han, *ACS Appl. Mater. Interfaces* **2022**, *14*, 35114.

[85] L. Lu, W. Ding, J. Liu, B. Yang, *Nano Energy* **2020**, *78*, 105251.

[86] L. Wu, Z. Jin, Y. Liu, H. Ning, X. Liu, Alamusi, N. Hu, **2022**, *11*, 1386.

[87] L. Wang, Y. Yu, X. Zhao, Z. Zhang, X. Yuan, J. Cao, W. Meng, L. Ye, W. Lin, G. Wang, *ACS Appl. Mater. Interfaces* **2022**, *14*, 46273.

[88] K. Tewatia, A. Sharma, M. Sharma, A. Kumar, *Mater. Today: Proc.* **2021**, *44*, 4548.

[89] A. Sood, M. Desseigne, A. Dev, L. Maurizi, A. Kumar, N. Millot, S. S. Han, *Small* **2023**, *19*, 2206401.

[90] H. GhaedRahmati, M. Frounchi, S. Dadbin, *Mater. Sci. Eng., B* **2022**, *276*, 115535.

[91] R. Fu, X. Zhong, C. Xiao, J. Lin, Y. Guan, Y. Tian, Z. Zhou, G. Tan, H. Hu, L. Zhou, C. Ning, *Nano Energy* **2023**, *114*, 108617.

[92] Z. Li, G. Li, X. Wang, Z. Zhao, *J. Mater. Sci. Technol.* **2024**, *172*, 228.

[93] Y. Li, R. Fu, Y. Guan, Z. Zhang, F. Yang, C. Xiao, Z. Wang, P. Yu, L. Hu, Z. Zhou, C. Ning, *ACS Biomater. Sci. Eng.* **2022**, *8*, 3078.

[94] Z. Liu, X. Wan, Z. L. Wang, L. Li, *Adv. Mater.* **2021**, *33*, 2007429.

[95] K. S. Ramadan, D. Sameoto, S. Evoy, *Smart Mater. Struct.* **2014**, *23*, 033001.

[96] S. Veeralingam, S. Badhulika, *Mater. Res. Bull.* **2022**, *150*, 111779.

[97] M. Shabani Samghabadi, A. Karkhaneh, A. A. Katbab, *Polym. Adv. Technol.* **2023**, *34*, 1367.

[98] I. Chiesa, C. De Maria, M. R. Ceccarini, L. Mussolin, R. Coletta, A. Morabito, R. Tonin, M. Calamai, A. Morrone, T. Beccari, L. Valentini, *ACS Appl. Mater. Interfaces* **2022**, *14*, 19253.

[99] Z. Wang, Y. Cong, J. Fu, *J. Mater. Chem. B* **2020**, *8*, 3437.

[100] J. Wu, T. Chen, Y. Wang, J. Bai, C. Lao, M. Luo, M. Chen, W. Peng, W. Zhi, J. Weng, J. Wang, *Biomedicines* **2022**, *10*, 1165.

[101] M. Ali, M. J. Bathaei, E. Istif, S. N. H. Karimi, L. Beker, *Adv. Healthcare Mater.* **2023**, *12*, 2300318.

[102] R. Wang, J. Sui, X. Wang, *ACS Nano* **2022**, *16*, 17708.

[103] C. Cui, Q. Fu, L. Meng, S. Hao, R. Dai, J. Yang, *ACS Appl. Bio Mater.* **2021**, *4*, 85.

[104] A. Miserez, J. C. Weaver, O. Chaudhuri, *J. Mater. Chem. B* **2015**, *3*, 13.

[105] X. Lin, X. Zhao, C. Xu, L. Wang, Y. Xia, *J. Polym. Sci.* **2022**, *60*, 2525.

[106] W. Xing, Y. Tang, *Nano Mater. Sci.* **2022**, *4*, 83.

[107] Z. Cui, W. Wang, L. Guo, Z. Liu, P. Cai, Y. Cui, T. Wang, C. Wang, M. Zhu, Y. Zhou, W. Liu, Y. Zheng, G. Deng, C. Xu, X. Chen, *Adv. Mater.* **2022**, *34*, 2104078.

[108] X. Song, C. Zhu, D. Fan, Y. Mi, X. Li, R. Z. Fu, Z. Duan, Y. Wang, R. R. Feng, *Polymers* **2017**, *9*, 638.

[109] G. Liu, Z. Lv, S. Batool, M.-Z. Li, P. Zhao, L. Guo, Y. Wang, Y. Zhou, S.-T. Han, *Small* **2023**, *19*, 2207879.

[110] W. Wang, J. Li, H. Liu, S. Ge, *Adv. Sci.* **2021**, *8*, 2003074.

[111] M. Pusnik, M. Imeri, G. Deppierraz, A. Bruinink, M. Zinn, *Sci. Rep.* **2016**, *6*, 20854.

[112] S. Naahidi, M. Jafari, M. Logan, Y. Wang, Y. Yuan, H. Bae, B. Dixon, P. Chen, *Biotechnol. Adv.* **2017**, *35*, 530.

[113] I. Porto, in *Polymerization*, Vol. 2750 (Ed.: A. de Souza Gomes), InTech, Rijeka, Croatia **2012**, Ch. 3.

[114] A. van Tonder, A. M. Joubert, A. D. Cromarty, *BMC Res. Notes* **2015**, *8*, 47.

[115] L. Sanders, R. Stone, K. Webb, T. Mefford, J. Nagatomi, *J. Biomed. Mater. Res. A* **2015**, *103*, 861.

[116] N. Batool, R. M. Sarfraz, A. Mahmood, M. Zaman, N. Zafar, A. Salawi, Y. Almoshari, M. Alshamrani, *Gels* **2022**, *8*, 190.

[117] R. Serra-Gómez, C. A. Dreiss, J. González-Benito, G. González-Gaitano, *Langmuir* **2016**, *32*, 6398.

[118] J. P. Ball, B. A. Mound, J. C. Nino, J. B. Allen, *J. Biomed. Mater. Res., Part A* **2014**, *102*, 2089.

[119] M. Xu, S. Wu, L. Ding, C. Lu, H. Qian, J. Qu, Y. Chen, *J. Mater. Chem. B* **2023**, *11*, 4318.

[120] M. Weber, H. Steinle, S. Golombek, L. Hann, C. Schlensak, H. P. Wendel, M. Avcı-Adalı, *Front. Bioeng. Biotechnol.* **2018**, *6*, 99.

[121] J. Ma, P. Yu, B. Xia, Y. An, *e-Polymers* **2019**, *19*, 594.

[122] M. Jurak, A. E. Wiącek, A. Ładniak, K. Przykaza, K. Szafran, *Adv. Colloid Interface Sci.* **2021**, *294*, 102451.

[123] B. P. Chan, K. W. Leong, *Eur. Spine J.* **2008**, *17*, 467.

[124] J. Saroia, W. Yanen, Q. Wei, K. Zhang, T. Lu, B. Zhang, *Bio-Des. Manuf.* **2018**, *1*, 265.

[125] Y. Zhang, Y. Liu, H.-Y. Ye, D.-W. Fu, W. Gao, H. Ma, Z. Liu, Y. Liu, W. Zhang, J. Li, G.-L. Yuan, R.-G. Xiong, *Angew. Chem., Int. Ed.* **2014**, *53*, 5064.

[126] W. Gao, L. Chang, H. Ma, L. You, J. Yin, J. Liu, Z. Liu, J. Wang, G. Yuan, *NPG Asia Mater.* **2015**, *7*, e189.

[127] I. Bergenti, *J. Phys. D: Appl. Phys.* **2022**, *55*, 033001.

[128] M. Dong, X. Wang, X.-Z. Chen, F. Mushtaq, S. Deng, C. Zhu, H. Torlakcik, A. Terzopoulou, X.-H. Qin, X. Xiao, J. Puigmartí-Luis, H. Choi, A. P. Pêgo, Q.-D. Shen, B. J. Nelson, S. Pané, *Adv. Funct. Mater.* **2020**, *30*, 1910323.

[129] C. R. Dumitrescu, I. A. Neacsu, R. Trusca, R. C. Popescu, I. Raut, M. Constantin, E. Andronescu, *Polymers* **2023**, *15*, 2446.

[130] C. P. Jiménez-Gómez, J. A. Cecilia, *Molecules* **2020**, *25*.

[131] H. Park, K. Park, W. S. Shalaby, *Biodegradable Hydrogels for Drug Delivery*, CRC Press, San Diego, CA, **1993**.

[132] L. Hu, P. L. Chee, S. Sugiarto, Y. Yu, C. Shi, R. Yan, Z. Yao, X. Shi, J. Zhi, D. Kai, H.-D. Yu, W. Huang, *Adv. Mater.* **2023**, *35*, 2205326.

[133] Y. Du, W. Du, D. Lin, M. Ai, S. Li, L. Zhang, *Micromachines* **2023**, *14*, 167.

[134] C. Chen, X. Bai, Y. Ding, I.-S. Lee, *Biomater. Res.* **2019**, *23*, 25.

[135] C. Wu, L. Shen, Y. Lu, C. Hu, Z. Liang, L. Long, N. Ning, J. Chen, Y. Guo, Z. Yang, X. Hu, J. Zhang, Y. Wang, *ACS Appl. Mater. Interfaces* **2021**, *13*, 52308.

[136] M. Levin, *Mol. Biol. Cell* **2014**, *25*, 3835.

[137] B. D. Manning, A. Toker, *Cell* **2017**, *169*, 381.

[138] R. Roskoski Jr, *Pharmacol. Res.* **2012**, *66*, 105.

[139] S. Ren, J. Chen, D. Duscher, Y. Liu, G. Guo, Y. Kang, H. Xiong, P. Zhan, Y. Wang, C. Wang, H. G. Machens, Z. Chen, *Stem Cell Res. Ther.* **2019**, *10*, 47.

[140] L. Roldan, C. Montoya, V. Solanki, K. Q. Cai, M. Yang, S. Correa, S. Orrego, *ACS Appl. Mater. Interfaces* **2023**, *15*, 43441.

[141] J. Wu, T. Chen, Y. Wang, J. Bai, C. Lao, M. Luo, M. Chen, W. Peng, W. Zhi, J. Weng, J. Wang, *Biomedicines* **2022**, *10*, 165.

[142] G. Li, Z. Li, Y. Min, S. Chen, R. Han, Z. Zhao, *Small* **2023**, *19*, 2302927.

[143] L. Roldan, C. Montoya, V. Solanki, K. Q. Cai, M. Yang, S. Correa, S. Orrego, *ACS Appl. Mater. Interfaces* **2023**, *15*, 43441.

[144] G. Song, L. Cheng, Y. Chao, K. Yang, Z. Liu, *Adv. Mater.* **2017**, *29*, 1700996.

[145] A. Kumar, A. Tan, J. Wong, J. C. Spagnoli, J. Lam, B. D. Blevins, N. G., L. Thorne, K. Ashkan, J. Xie, H. Liu, *Adv. Funct. Mater.* **2017**, *27*, 1700489.

[146] Z. Zhou, J. Song, L. Nie, X. Chen, *Chem. Soc. Rev.* **2016**, *45*, 6597.

[147] S. Chen, P. Zhu, L. Mao, W. Wu, H. Lin, D. Xu, X. Lu, J. Shi, *Adv. Mater.* **2023**, *35*, 2208256.

[148] S. Wang, X. Lv, Y. Su, Z. Fan, W. Fang, J. Duan, S. Zhang, B. Ma, F. Liu, H. Chen, Z. Geng, H. Liu, *Small* **2019**, *15*, 1804593.

[149] D. Yu, Z. Liu, J. Zhang, S. Li, Z. Zhao, L. Zhu, W. Liu, Y. Lin, H. Liu, Z. Zhang, *Nano Energy* **2019**, *58*, 695.

[150] Y. Wang, S. Wang, Y. Meng, Z. Liu, D. Li, Y. Bai, G. Yuan, Y. Wang, X. Zhang, X. Li, X. Deng, *Nat. Commun.* **2022**, *13*, 4419.

[151] Y. Zhang, S. Chen, Z. Xiao, X. Liu, C. Wu, K. Wu, A. Liu, D. Wei, J. Sun, L. Zhou, H. Fan, *Adv. Healthcare Mater.* **2021**, *10*, 2100695.

[152] P. Wang, Q. Tang, L. Zhang, M. Xu, L. Sun, S. Sun, J. Zhang, S. Wang, X. Liang, *ACS Nano* **2021**, *15*, 11326.

[153] J. Lei, C. Wang, X. Feng, L. Ma, X. Liu, Y. Luo, L. Tan, S. Wu, C. Yang, *Chem. Eng. J.* **2022**, *435*, 134624.

[154] Y. Wang, X. Wen, Y. Jia, M. Huang, F. Wang, X. Zhang, Y. Bai, G. Yuan, Y. Wang, *Nat. Commun.* **2020**, *11*, 1328.

[155] P. Zhu, Y. Chen, J. Shi, *Adv. Mater.* **2020**, *32*, 2001976.

[156] T. Glaser, V. F. Arnaud Sampaio, C. Lameu, H. Ulrich, *Sem. Cell Dev. Biol.* **2019**, *95*, 25.

[157] A. B. Toth, A. K. Shum, M. Prakriya, *Cell. Calcium* **2016**, *59*, 124.

[158] X. Sun, F. Yao, J. Li, *J. Mater. Chem. A* **2020**, *8*, 18605.

[159] D. Zhang, B. Ren, Y. Zhang, L. Xu, Q. Huang, Y. He, X. Li, J. Wu, J. Yang, Q. Chen, Y. Chang, J. Zheng, *J. Mater. Chem. B* **2020**, *8*, 3171.

[160] G. Li, C. Li, G. Li, D. Yu, Z. Song, H. Wang, X. Liu, H. Liu, W. Liu, *Small* **2022**, *18*, 2101518.

[161] S. D. Mahapatra, P. C. Mohapatra, A. I. Aria, G. Christie, Y. K. Mishra, S. Hofmann, V. K. Thakur, *Adv. Sci.* **2021**, *8*, 2100864.

[162] F. Yang, J. Li, Y. Long, Z. Zhang, L. Wang, J. Sui, Y. Dong, Y. Wang, R. Taylor, D. Ni, W. Cai, P. Wang, T. Hacker, X. Wang, *Science* **2021**, *373*, 337.

[163] H. S. Wang, S. K. Hong, J. H. Han, Y. H. Jung, H. K. Jeong, T. H. Im, C. K. Jeong, B.-Y. Lee, G. Kim, C. D. Yoo, K. J. Lee, *Sci. Adv.* **7**, eabe5683.

[164] P.-C. Lee, Y.-L. Hsiao, J. Dutta, R.-C. Wang, S.-W. Tseng, C.-P. Liu, *Nano Energy* **2021**, *82*, 105702.

[165] N.-I. Kim, J. Chen, W. Wang, M. Moradnia, S. Pouladi, M.-K. Kwon, J.-Y. Kim, X. Li, J.-H. Ryou, *Adv. Funct. Mater.* **2021**, *31*, 2008242.

[166] R. Mestre, J. Fuentes, L. Lefax, J. Wang, M. Guix, G. Murillo, R. Bashir, S. Sánchez, *Adv. Mater. Technol.* **2023**, *8*, 2200505.

[167] H. Cui, D. Yao, R. Hensleigh, H. Lu, A. Calderon, Z. Xu, S. Davaria, Z. Wang, P. Mercier, P. Tarazaga, X. Zheng, *Science* **2022**, *376*, 1287.

[168] X. Gao, J. Yang, J. Wu, X. Xin, Z. Li, X. Yuan, X. Shen, S. Dong, *Adv. Mater. Technol.* **2020**, *5*, 1900716.

[169] E. Chen, Y. Yang, M. Li, B. Li, G. Liu, W. Mu, R. Yin, *Adv. Sci.* **2023**, *10*, 2300673.

[170] M. Han, H. Wang, Y. Yang, C. Liang, W. Bai, Z. Yan, H. Li, Y. Xue, X. Wang, B. Akar, H. Zhao, H. Luan, J. Lim, I. Kandela, G. A. Ameer, Y. Zhang, Y. Huang, J. A. Rogers, *Nat. Electron.* **2019**, *2*, 26.



**Chi Zhang** is currently a postdoctoral research associate under the supervision of Professor Lin Dong at New Jersey Institute of Technology. He received his Ph.D. from Technical Institute of Physics and Chemistry, Chinese Academy of Sciences. His research interests include functional nanomaterials and flexible electronics for sensing and energy harvesting applications.



**Sun Hwa Kwon** is a Ph.D. student under the supervision of Professor Lin Dong at New Jersey Institute of Technology. She received her undergraduate and M.S. degrees from The Cooper Union for the Advancement of Science and Art. Her research interests include nanofibers, specifically piezoelectric nanofibers created using the electrospinning fabrication method, and biomedical devices, such as cardiac devices.



**Lin Dong** is an assistant professor at Department of Mechanical & Industrial Engineering at New Jersey Institute of Technology. She received her Ph.D. from Stevens Institute of Technology, where she was awarded Innovation and Entrepreneurship Doctoral Fellowship. She was a research associate at Thayer School of Engineering at Dartmouth College. Her research interests include nanomaterials and nanofabrication technology, flexible electronics, as well as energy harvesting and sensing devices for biomedical applications.